

Analysis of bank leverage via dynamical systems and deep neural networks

Fabrizio Lillo* Giulia Livieri† Stefano Marmi‡
Anton Solomko§ Sandro Vaienti¶

13 April 2021

Abstract

We consider a model of a simple financial system consisting of a leveraged investor that invests in a risky asset and manages risk by using Value-at-Risk (VaR). The VaR is estimated by using past data via an adaptive expectation scheme. We show that the leverage dynamics can be described by a dynamical system of slow-fast type associated with a unimodal map on $[0, 1]$ with an additive heteroscedastic noise whose variance is related to the portfolio rebalancing frequency to target leverage. In absence of noise the model is purely deterministic and the parameter space splits in two regions: (i) a region with a globally attracting fixed point or a 2-cycle; (ii) a dynamical core region, where the map could exhibit chaotic behavior. Whenever the model is randomly perturbed, we prove the existence of a unique stationary density with bounded variation, the stochastic stability of the process and the almost certain existence and continuity of the Lyapunov exponent for the stationary measure. We then use deep neural networks to estimate map parameters from a short time series. Using this method, we estimate the model in a large dataset of US commercial banks over the period 2001–2014. We find that the parameters of a substantial fraction of banks lie in the dynamical core, and their leverage time series are consistent with a chaotic behavior. We also present evidence that the time series of the leverage of large banks tend to exhibit chaoticity more frequently than those of small banks.

Keywords: leverage cycles, risk management, systemic risk, random dynamical systems, unimodal maps, Lyapunov exponents, neural networks.

2020 Mathematics Subject Classification: primary 91G80, 34F05; secondary 37H15, 62M45.

*Dipartimento di Matematica, Università di Bologna and Scuola Normale Superiore, Pisa, Italy. Email address: fabrizio.lillo@unibo.it

†Scuola Normale Superiore, Pisa, Italy. Email address: giulia.livieri@sns.it

‡Scuola Normale Superiore, Pisa, Italy. Email address: stefano.marmi@sns.it

§Scuola Normale Superiore, Pisa, Italy. Email address: solomko.anton@gmail.com

¶Aix Marseille Université, Université de Toulon, CNRS, CPT, 13009 Marseille, France. Email address: vaienti@cpt.univ-mrs.fr

Contents

1	Introduction	2
2	From the structural model to the dynamical system	8
3	The mathematical model	11
3.1	Unimodal maps	12
3.2	Markov chains	15
3.3	Coupling with a stochastic process	16
3.4	The leverage model	17
3.5	Random transformations	19
4	Stationary measure	20
4.1	Existence	21
4.2	Uniqueness	23
5	Stochastic stability	24
6	Lyapunov exponent	27
6.1	Average Lyapunov exponent	27
6.2	Continuity of the Lyapunov exponent	29
6.3	Random Lyapunov exponent and random entropy	32
7	Numerical results	33
7.1	Bifurcation diagram	33
7.2	Lyapunov exponent	34
8	Estimating the map parameters via deep neural networks	34
9	Chaos in real bank leverage time series	38
9.1	Data set	38
9.2	Estimation via neural networks	39
9.3	Classification via the Chaos Decision Tree Algorithm	42
10	Conclusions	43
11	Acknowledgements	44
A	The Chaos Decision Tree Algorithm	44
A.1	Simulations	45

1 Introduction

Leverage is one of the most important and controversial concepts in finance. On one side, borrowing is essential in many economic activities, while, on the other, it is intrinsically connected with risk. Concerning this last point, the

pro-cyclical nature of leverage has been highlighted and studied in the recent literature (see, e.g., [30, 2, 35, 3, 1, 50], among many others). Specifically, [2] and [3] argued that when assets are evaluated at *fair value*, an increase in market prices of assets decreases the so-called “quasi-market leverage ratio” – roughly the ratio of total assets to equity capital – and this leaves room to build up debt for banks that operate through leverage or Value at Risk¹ (VaR) targeting. The empirical findings in [2] and [3] show that cycles of expansion (contraction) in the banks’ balance sheet size go hand in hand with increases (decreases) in leverage (i.e., leverage is pro-cyclical); a behavior that has been witnessed since the 1960s but exacerbated during 2007–2009 financial crisis. The creation of negative externalities in financial markets because VaR model’s widespread use has been put forward in e.g., [51, 26, 41]. It is shown that it can create market instability and result in what has been called by [27] as *endogenous risk*, that is, the systemic risk caused and amplified by the system itself rather than being the result of an exogenous shock. Indeed, because of the imposed VaR capital requirements, banks are forced to reduce their positions when the risk exceeds these limits. Since the VaR of the trading portfolio increases when the volatility goes up, banks are forced to reduce their positions rapidly, and because of these fire sales, the price can drop abruptly. This leads to a new drop in prices and likely increases volatility, which triggers (further) portfolio reductions. This mechanism creates an exceptionally threatening environment if many banks hold similar positions and use the same VaR model to manage their risk since they are forced to sell the same assets contemporaneously, leading to a destabilizing spiral. Finally, to implement the VaR constraint (as well as any risk management mechanism), banks must estimate both the riskiness of the investments and their dependencies. Since the estimation of risk is typically done using historical data, additional feedback is created between past and future risks, creating new threats for the systemic stability of financial markets.

Understanding and modeling the leverage dynamics is therefore of paramount importance. Some recent papers [8, 25, 44] have proposed stylized agent-based models of financial institutions that lead to a dynamical system evolution for the leverage. By using *numerical methods*, they also show that in some parameters regime the leverage dynamics becomes chaotic via a cascade of period doubling bifurcations². The map describing some of these models also contains a noise component, describing the uncertainty naturally present in financial institutions’ decision process. For example, optimal leverage depends on portfolio risk, which is typically estimated with statistical methods on past observations and these estimations are naturally modeled as random variables. In this paper, we address three important questions related to this approach (to be discussed below): (1) What are the mathematical properties (existence and uniqueness of stationary measure, stochastic stability, Lyapunov exponent, etc.) of the noisy deterministic maps emerging from these models? (2) Is it possible to reliably

¹The Value at Risk measures the maximum loss that an asset portfolio may suffer over a specific horizon and with a given level of confidence.

²Other works that analyze systemic risk problems through tools from dynamical system theory are, e.g. [23, 24, 52, 20, 9], to cite only a few.

estimate the map parameters from short time series as those in publicly available datasets of banks balance sheets? (3) Is there evidence of chaotic behavior in the leverage dynamics of real banks?

We consider a simple agent-based financial system where the mechanisms described above are present. Our starting point is a simplified version of the model proposed in [44], which in turn builds on [25], to the case of one bank and one asset. As [44] shows numerically, the dynamics describing the financial leverage displays a period-doubling bifurcation cascade resulting in chaotic behaviour (as measured with the computation of the Lyapunov exponent). This happens either when the parameter of the VaR constraint or the memory used by the banks to estimate volatility from past data vary. These findings, while suggestive, are however not rigorously proved in [44]. More importantly, the mathematical properties of this family of models, i.e. where a deterministic map is perturbed by a heteroscedastic additive noise (arising from the coupling with a faster random dynamics), are not known in general. In the simplified model, the system is composed of a representative leveraged investor (a bank) that invests in a risky asset; the bank's risk management consists of two components. First, the bank estimates the future volatility (the risk) of its investment in the risky asset using past market data. Second, the bank uses the estimated volatility to set its desired leverage. However, the bank faces a Value-at-Risk (VaR) capital requirement policy which implies a constraint for the financial leverage $\lambda_t := A_t/E_t$, where A_t indicates the assets of the bank at time t , whereas E_t the liabilities. The bank is allowed a maximum leverage $\bar{\lambda}_t$ which is a function of its own perceived risk. The representative bank updates its expectation of risk at time intervals of unitary length, say $(t, t + 1]$ with $t \in \mathbb{Z}$, and, accordingly, it makes new decisions about the leverage. This process defines the *slow* component of the model. Moreover, the model assumes that over the unitary time interval $(t, t + 1]$ representative bank re-balances its portfolio to target the leverage without changing the risk expectations. The re-balancing takes place in n time sub-intervals within $(t, t + 1]$. The time scale $1/n$, with $n \in \mathbb{N}$, characterizes the *fast* component of the model. In particular, the slow variables evolve in time as a function of averages over the fast variables. In summary, the considered model is a discrete-time slow-fast dynamical system ([29] and [14]). Starting from this model, in this paper we make three main contributions.

First, we show that the dynamics of leverage in our model follows, under suitable approximation, a deterministic unimodal map on $[0, 1]$ perturbed with additive and heteroscedastic noise. The variance of the noise is related to the frequency of portfolio rebalancing to target leverage. In particular, the parameter space of this deterministic map has two regions: (i) a region where the map has a globally attracting fixed point or a 2-cycle; (ii) the so-called *dynamical core* region, where the map can exhibit chaotic behavior. In order to study the mathematical properties of the map rigorously, we consider a more general class of maps and describe the leverage dynamic utilizing a Markov chain parametrized by the *rebalance time* n ; we will study the regime of finite n , as well as the limit for $n \rightarrow \infty$. Although the stability of Markov chains is relatively well studied (see e.g., [17] or [46] and references therein), some specific properties of

the stochastic kernel that defines our model do not allow us to apply general results available; for instance, we do not know if our chain is Harris recurrent. We instead exploit the unimodal dynamics of the deterministic map. Perturbations of unimodal maps with uniform additive noise were studied in [12], [13]. As far as we know, the Markov chains with the kind of heteroscedastic noise we introduce are apparently new; see [32] for another type of heteroscedastic nonlinear autoregressive process applied to financial time series. To handle with them, we look at the Markov operator's spectral properties on suitable Banach spaces and prove the quasi-compactness of such an operator. This allows us to obtain many rigorous results. In particular, we get finitely many stationary measures with bounded variation densities. The stationary measure's uniqueness is achieved when the chain perturbs the unimodal map which is either topologically transitive or admits an attracting periodic orbit; such maps correspond to a major part of the parameter space. From a financial point of view, should the stationary measure not be unique, it would imply that, depending on the initial conditions, different banks could experience completely different dynamics, corresponding to different stationary measures. When this occurs in physical systems one speaks of phase transitions and of coexistence of different mutually singular states. In our case, this would imply, for instance, that policy measures could not be universal. We also show the weak convergence of the unique stationary measure to the invariant measure of the unimodal map. We point out that this step is particularly delicate since the stochastic kernel becomes singular in the limit of large n . It is well known that given a continuous Markov chain which perturbs a given map T as in our setting, one could construct a sequence of random transformations close to T and therefore replace the deterministic orbit of T with a random orbit given by the concatenation of the maps randomly chosen in the sequence. This construction is formally possible under general assumptions, but it is challenging to get "representations by special classes of transformations" as Y. Kifer pointed out in [37]. We provide an explicit construction of those transformations and show their closeness with the unimodal map; we believe this inference from the Markov chain to the random transformations is interesting and illustrates very well the way the Markov chain moves randomly the states of the system. In particular, our random maps are obtained by adding to the unimodal map T an additive term which also depends on the state variable, and this motivates the attribute of heteroscedastic we gave to our noise. Once we dispose of the stationary measure, we can define an average Lyapunov exponent by integrating the logarithm of the derivative of the unimodal map T with respect to such a measure; this definition is suitable for the Markov chain approach. By switching to random transformations, one can define the Lyapunov exponent of the cocycle. We show numerically that the two approaches are asymptotically equivalent and prove that the average exponent converges to the Lyapunov exponent of T in the limit of large n , as a consequence of the stochastic stability. We finally show that the average Lyapunov exponent depends continuously on the Markov chain parameters, and relate it to the different chaotic behavior of the unperturbed unimodal map.

One of the purposes of the present work was to rigorously establish the

possibility of chaotic behaviour in leverage time series of banks, as well as to detect it in financial datasets. For this reason we started from the parametric slow-fast model of [44] and looked at the corresponding Lyapunov exponent. We remind that for deterministic systems, the Lyapunov exponents characterize the divergence of nearby orbits, allowing to distinguish between regular and chaotic dynamics. In the presence of the noise, our model becomes intrinsically stochastic, in particular the Markov chain will mix exponentially fast, see section 6.3. Nevertheless the average Lyapunov exponent still allows us to discriminate periodic and chaotic behaviours: it is negative when we perturb a contracting map (and then the realizations of the process fluctuate around the fixed point), and it becomes positive by perturbing the dynamical core region. In both cases the distribution of the realizations in the state space is governed by the unique absolutely continuous stationary measure. We prove that both behaviours, chaotic and periodic, are present in the parameter space and we actually observe both regimes in the real data. This justifies our claims about chaotic dynamics of the leverage.

Indeed, in our third contribution (to be detailed below) we will detect possible chaos in banks' leverage dynamics. As said, for the stochastic stability and the Lyapunov exponent we mainly discuss the relation between finite n (thus noisy system) and infinite n (purely deterministic system). Thus our results indicate in which sense what we learn for a noisy system is informative about the deterministic backbone. In our empirical analysis we will do not study or use directly neither the stationary measure nor the Lyapunov exponent (mainly because we have very short time series), however the "continuity" we observe from finite to infinite n suggests that the properties we observe empirically for finite n are informative of the underlying deterministic dynamics.

The paper's second contribution concerns a methodology to infer the parameters of the noisy map from short empirical time series. It is indeed interesting to ask if there is evidence of chaotic behavior in the leverage dynamics of real banks. We claim that applying the maximum likelihood estimation is not feasible for two reasons. First, the likelihood function is highly non-convex so that standard optimization methods may perform poorly. Second, although the likelihood function for the process itself can be written explicitly, it may happen that in many cases we observe only a certain iterate of the process, e.g., we observe only one slow time scale portfolio decision event out of two. Therefore we propose to use a powerful deep learning technique known as Convolutional Neural Network (CNN) ([40]) to estimate the parameters of the map. More precisely, our CNN takes as input the one-dimensional time-series and gives as output the map's corresponding parameters. We train the CNN via extensive simulations of the model, considering different regions of the parameter space. The robustness of the trained model is validated by its prediction of parameters performance in a huge testing set. Results show the merit of using our proposed CNN architecture to estimate the parameters. Importantly, being based only on simulations, the NN-based approach can also work for partial observations. Without attempting to review the literature of parameter estimation of the dynamical system via NN, we only provide here a few key references to posi-

tion our contribution. [47] employed multi-layer NN and recurrent networks to identify and control nonlinear deterministic dynamical systems. Artificial NN have been used in [42] and [53] in a similar framework. Batch and recursive prediction error estimation algorithm have been derived for a NN model with a single hidden layer in [22] and [21] for the identification of noisy discrete-time nonlinear dynamical systems.

The third contribution is the empirical analysis of real banks leverage time series. Assuming the proposed unimodal map with heteroscedastic noise as data generating process for the banks' leverage, we estimate the parameters on quarterly data of about 5,000 US Commercial Banks provided by the Federal Financial Institutions Examination Council (FFIEC) via the proposed CNN architecture. We have at our disposal a time period going from March 2001 to December 2014, for a total of 59 quarters. Remarkably, we find that the parameters of a sizable fraction of banks lie in the map's dynamical core and that the large banks' leverage tends to be more chaotic than one of the small ones. As a robustness check, identifying chaotic/periodic behavior is tested by following a non-parametric approach. In this latter case, the map is not specified and estimators of indicators (such as the Lyapunov exponent [59]), which assume different values in the two regimes, are used to discriminate them from a finite length time series. We use a very recent algorithm dubbed Chaos Decision Tree Algorithm [57] which combines several tools into an automated processing pipeline that can detect the presence (or absence) of chaos in noisy recordings, even for difficult edge cases. We apply the Chaos Decision Tree Algorithm to our data set. Remarkably, the results corroborate the CNN approach's findings concerning the chaotic behavior for a significant subset of typically large banks.

Outline of the paper. In Section 2 we present the financial model of a representative bank managing its leverage. We show that the model leads to a slow-fast deterministic-random dynamical system which can be recasted into a unimodal deterministic map with heteroscedastic noise. In order to analyze it rigorously, in Section 3 we recall some facts about unimodal maps and Markov chains and then define the class of chains that we study. We also represent our model in terms of random transformations. In Section 4 and 5 we show the existence and uniqueness of an absolutely continuous stationary measure and establish its convergence to the invariant measure of the deterministic map. This allows us to define the Lyapunov exponent and prove its continuity with respect to the model parameters in Section 6. We also discuss chaotic indicators naturally arising from the random maps representation of the process. The last part of the paper concerns numerical and empirical analyses. Specifically, Section 7 presents some numerical investigations of the bifurcation diagram and Lyapunov exponent of the map. Section 8 proposes an estimation method of the map based on the use of deep neural networks and Section 9 presents an empirical application to a large set of leverage time series of US banks, showing evidence of chaotic behavior. Finally, in Section 10 we draw some conclusions and outline some potential extensions of our work.

2 From the structural model to the dynamical system

The stylized model of the leverage dynamics we are going to present is a special case of the model of [44] (which in turn builds on [25]) restricted to the case of a single (representative) financial institution and of a single investment asset. We present below this model and show how, under suitable approximation, the resulting dynamics of leverage follows a deterministic map with additive and heteroscedastic noise. The mathematical properties of such map are studied in the next sections.

In the model, a representative financial institution (hereafter a bank) takes investment decisions at discrete times $t \in \mathbb{Z}$ (the slow time scale). At each time the bank's balance sheet is characterized by the asset A_t and equity E_t , which together define the leverage $\lambda_t := A_t/E_t$. The bank wants to maximize leverage (by taking more debt) to increase profits, but regulation constrains the bank's Value-at-Risk (VaR) in such a way that

$$\lambda_t = \frac{1}{\alpha \sigma_{e,t}},$$

where α depends on the return distribution and VaR constraint³. $\sigma_{e,t}$ is the expected volatility at time t of the asset, which in this simple model is composed by a representative risky investment. Thus at each time t the bank recomputes $\sigma_{e,t}$ and chooses λ_t . Then in the interval $[t, t+1]$ the bank trades the risky investment to keep the leverage close to the target λ_t . The trading process occurs on the points of a grid obtained by subdividing $[t, t+1]$ in n subintervals of length $1/n$ (the fast time scale). The dynamics of the investment return can be written as

$$r_{t+k/n} = \varepsilon_{t+k/n} + e_{t+(k-1)/n}, \quad k = 1, 2, \dots, n, \quad (1)$$

where $\varepsilon_{t+k/n}$ and $e_{t+(k-1)/n}$ are, respectively, the exogenous and endogenous component of the return. The former is a white noise term with variance σ_ε^2 , while the latter depends on the banks' demand for the risky investment in the previous step. For each bank, the demand for the risky investment at time $t+k/n$ is the difference between the target value of A_t to reach λ_t and its actual value. Since the bank's asset is composed by the risky investment, an investment return $r_{t+k/n}$ modifies A_t and the bank trades at each grid point to reach the target leverage. It is possible to show (see [25, 44]) that to achieve this, at each time $t+k/n$ the bank's demand for the risky investment is

$$D_{t+k/n} = (\lambda_t - 1)A_{t+(k-1)/n}^* r_{t+k/n},$$

where $A_{t+(k-1)/n}^*$ is the target asset size in the previous step. If there are M identical banks, the aggregated demand is $MD_{t+k/n}$. The endogenous component

³For example, if returns are Gaussian and the probability of VaR is 5%, it is $\alpha = 1.64$.

of returns $e_{t+k/n}$ is determined by the aggregated demand by the equation

$$e_{t+k/n} = \frac{1}{\gamma} \frac{MD_{t+k/n}}{C_{t+k/n}},$$

where $C_{t+k/n} = MA_{t+(k-1)/n}^*$ is a proxy of the market capitalization of the risky asset and γ is a parameter measuring the investment liquidity. Using the above expression, it is

$$e_{t+k/n} = \frac{\lambda_t - 1}{\gamma} e_{t+(k-1)/n} = \phi_t e_{t+(k-1)/n}$$

and thus in the period $[t, t+1]$ the return $r_{t+k/n}$ follows an AR(1) process with autoregression parameter $\phi_t = (\lambda_t - 1)/\gamma$ and idiosyncratic variance σ_e^2 .

To close the model, we specify how the bank forms expectations $\sigma_{e,t}$ on future volatility at time t . We assume that bank uses adaptive expectations, which implies that

$$\sigma_{e,t}^2 = \omega \sigma_{e,t-1}^2 + (1 - \omega) \hat{\sigma}_{e,t}^2,$$

where $\omega \in [0, 1]$ is a parameter weighting between the expectation at $t - 1$ and the estimation $\hat{\sigma}_{e,t}^2$ of volatility obtained by the return data in $[t - 1, t]$. As done in practice, this is obtained by estimating the sample variance of the returns in $[t - 1, t]$, i.e.

$$\begin{aligned} \hat{\sigma}_{e,t}^2 &= \widehat{\text{Var}} \left[\sum_{k=1}^n r_{t-1+k/n} \right] \\ &= \left(1 + 2 \frac{\hat{\phi}_{t-1}(1 - \hat{\phi}_{t-1}^n)}{1 - \hat{\phi}_{t-1}} - 2 \frac{(n\hat{\phi}_{t-1} - n - 1)\hat{\phi}_{t-1}^{n+1} + \hat{\phi}_{t-1}}{n(1 - \hat{\phi}_{t-1})^2} \right) \frac{n\hat{\sigma}_e^2}{1 - \hat{\phi}_{t-1}^2}, \end{aligned} \quad (2)$$

where the last expression gives the aggregated variance of an AR(1) process as a function of the AR estimated parameters $\hat{\phi}_{t-1}$ and $\hat{\sigma}_e^2$. In the following we will assume that these are the MLE estimators. We remind that when n is large, $\hat{\phi}_{t-1}$ is a Gaussian distributed variable with mean ϕ_{t-1} and variance $(1 - \phi_{t-1}^2)/n$.

In conclusion, the leverage dynamics is described by the following equations:

$$\begin{cases} \lambda_t = \left(\omega \frac{1}{\lambda_{t-1}^2} + (1 - \omega) \alpha^2 \widehat{\text{Var}}[\sum_{k=1}^n r_{t-1+k/n}] \right)^{-1/2}, \\ r_s = \phi_{t-1} r_{s-1/n} + \epsilon_s, \quad s = t - 1 + k/n, \quad k = 1, 2, \dots, n, \end{cases} \quad (3)$$

Since slow variables evolve depending on averages of the fast variables, the model is a *slow-fast deterministic-random dynamical system*. By using the expression above for the variance, we can rewrite the equation for the slow component only as

$$\lambda_t = \left(\omega \frac{1}{\lambda_{t-1}^2} + (1 - \omega) \alpha^2 \hat{\sigma}_{e,t}^2 \right)^{-1/2},$$

where the estimator $\hat{\sigma}_{e,t}^2$ can be seen as a stochastic term depending on λ_{t-1} and whose variance goes to zero when $\mathfrak{n} \rightarrow \infty$.

If \mathfrak{n} is large, the above map reduces to

$$\lambda_t = \left(\omega \frac{1}{\lambda_{t-1}^2} + \frac{(1-\omega)\alpha^2 \mathfrak{n} \hat{\sigma}_\epsilon^2}{(1-\hat{\phi}_{t-1})^2} \right)^{-1/2},$$

and using the relation $\phi_t = \frac{\lambda_t - 1}{\gamma}$, the map becomes

$$\phi_t = -\frac{1}{\gamma} + \frac{1}{\gamma} \left(\frac{\omega}{(1+\gamma\phi_{t-1})^2} + \frac{(1-\omega)\alpha^2 \mathfrak{n} \hat{\sigma}_\epsilon^2}{(1-\hat{\phi}_{t-1})^2} \right)^{-1/2}. \quad (4)$$

When changing \mathfrak{n} also σ_ϵ^2 changes, since the AR(1) can be seen as the discretization of a continuous time stochastic process (namely an Ornstein-Uhlenbeck process). A simple scaling argument shows that the quantity $\Sigma_\epsilon = \sigma_\epsilon^2 \mathfrak{n}$ is instead constant and independent from the discretization step $1/\mathfrak{n}$. In the limit $\mathfrak{n} \rightarrow \infty$, it is $\hat{\phi}_t \rightarrow \phi_t$, thus the above map becomes purely deterministic⁴. The map in this case has a fixed point $\phi^* = \frac{1-\alpha\sqrt{\Sigma_\epsilon}}{1+\alpha\gamma\sqrt{\Sigma_\epsilon}}$. By replacing this condition in (2) and assuming that the risky asset is very liquid ($\gamma \gg 1$), the map becomes

$$\phi_t \simeq \left(\frac{\omega}{\phi_{t-1}^2} + \left(\frac{1-\phi^*}{\phi^*} \right)^2 \frac{1-\omega}{(1-\hat{\phi}_{t-1})^2} \right)^{-1/2}. \quad (5)$$

Since in the large \mathfrak{n} limit the ML estimator $\hat{\phi}_{t-1}$ is a Gaussian variable with mean ϕ_{t-1} and variance $(1-\phi_{t-1}^2)/\mathfrak{n}$, we can write

$$\hat{\phi}_{t-1} = \phi_{t-1} + \eta_{t-1},$$

where $\eta_{t-1} \sim \mathcal{N}(0, (1-\phi_{t-1}^2)/\mathfrak{n})$. If the noise η_{t-1} is small (i.e. \mathfrak{n} is large), we can perform a series expansion, obtaining

$$\phi_t \simeq \frac{|\phi_{t-1}(1-\phi_{t-1})|}{\sqrt{b\phi_{t-1}^2 + \omega(1-\phi_{t-1})^2}} (1 + \zeta_{t-1}), \quad (6)$$

where $b = b(\omega, \phi^*)$ is given by

$$b = (1-\omega) \left(\frac{1-\phi^*}{\phi^*} \right)^2 \quad (7)$$

and the noise term

$$\zeta_{t-1} = \frac{-b\phi_{t-1}^2}{(1-\phi_{t-1})(b\phi_{t-1}^2 + \omega(1-\phi_{t-1})^2)} \eta_{t-1}.$$

⁴This is the deterministic skeleton, whose properties are discussed in detail in [44].

In this approximation, the map can be seen as deterministic map with additive, but heteroscedastic, noise

$$\phi_{t+1} = T(\phi_t; \theta) + \sigma(\phi_t; \theta)\epsilon_t, \quad (8)$$

where $\epsilon_t \sim \mathcal{N}(0, 1)$ and θ is a vector of parameters. In our setting $\theta = (b, \omega, n)$ and the deterministic map T does not depend on n . Specifically,

$$T(\phi_t; \theta) = \frac{|\phi_t(1 - \phi_t)|}{\sqrt{b\phi_t^2 + \omega(1 - \phi_t)^2}} \quad (9)$$

and

$$\sigma(\phi_t; \theta) = \frac{b\phi_t^3 \sqrt{1 - \phi_t^2}}{\sqrt{n}(b\phi_t^2 + \omega(1 - \phi_t)^2)^{3/2}}. \quad (10)$$

The map T is represented in Fig. 1. The term under square root is always positive, since so are ω and b .

In the next sections we develop a rigorous mathematical theory of additive maps with heteroscedastic noise as in (8). In particular, we will study the existence of a stationary measure, the stochastic stability, and the Lyapunov exponent for this class of models, having in mind our main example of (9) and (10) coming from the financial application. It is worth noting, however, that our results remain valid for any noise ϵ_t in (8), not only Gaussian; see Section 3.3. Then in Section 8 we will present an estimation method for the map and in Section 9 we will present the empirical analysis on real leverage time series.

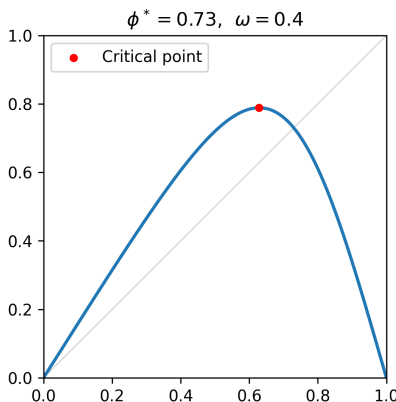


Figure 1: Plot of the deterministic component $T(\phi)$, $\phi^* = 0.73$, $\omega = 0.4$ ($b = 0.082$).

3 The mathematical model

As we explained in the previous section, we model the dynamics of a financial system where two time scales are present: a *slow time scale* where risk expectations (thus portfolios) are updated at unit times t , and a *fast time scale*, between

$t - 1$ and t , during which banks rebalance portfolios n times. Since slow variables evolve depending on averages of the fast variables, the model is a *slow-fast deterministic-random dynamical system*. The evolution of the slow component is described by equations (5) and (8). Notice that since the distribution of ϕ_t only depends on ϕ_{t-1} , both processes are (continuous state) Markov chains. In this section, we define some tools that we later use to analyse the model.

3.1 Unimodal maps

Our process is constructed by perturbing with a heteroscedastic additive noise a deterministic unimodal map T of the unit interval $I = [0, 1]$. We now describe the class of unimodal maps T we will consider, with (9) being its representative.

We will refer to the class of unimodal maps studied in [13]; they enjoy a series of ergodic properties which allow us to establish rigorous results for the problem we deal with.

We therefore consider unimodal maps $T: I \rightarrow I$ of class C^4 with $T(0) = T(1) = 0$ and with a non-degenerate critical point⁵ at $c: T'(c) = 0$. The map T is strictly increasing on $[0, c)$ and strictly decreasing on $(c, 1]$. Moreover, we suppose that T satisfies the following assumptions:

$$(A1) \quad T \text{ has negative Schwarzian derivative: } S(T) = \frac{T'''}{T'} - \frac{3}{2} \left(\frac{T''}{T'} \right)^2 < 0,$$

$$(A2) \quad \Delta := T(c) < 1,$$

$$(A3) \quad \text{the critical point is quadratic: } T''(c) \neq 0,$$

$$(A4) \quad |T^k(c) - c| \geq e^{-\alpha k} \text{ for all } k \geq k_0,$$

$$(A5) \quad |(T^k)'(\Delta)| \geq \lambda_c^k \text{ for all } k \geq k_0,$$

where $k_0 \geq 1$, $1 < \lambda_c < 2$, and $\alpha > 0$ with $e^{2\alpha} < \sqrt{\lambda_c}$ are fixed constants.

According to the theory of unimodal maps (see for instance the review [56]), we have the following classification:

(C1) If $\Delta \leq c$, then there exists a globally attracting fixed point.

(C2) If $c < T(\Delta) < \Delta$, then there is a globally attracting fixed point or a 2-cycle in (c, Δ) .

(C3) If $T(\Delta) < c < \Delta$, we can reduce the study to the so-called *dynamical core* $[T(\Delta), \Delta]$, which is mapped onto itself and absorbs all initial conditions (except 0 which is a fixed point).

Following this classification, we will say that T is **periodic** if there is a globally attracting fixed point or a globally attracting cycle. Recall that a map T on a topological space X is called *topologically transitive* if for all nonempty open sets $U, V \subset X$, there exists n such that $T^{-n}U \cap V \neq \emptyset$. We will say that T is **chaotic** if, in addition to above assumptions (A1)–(A5),

⁵The critical point for (9) is $c = (1 + \sqrt[3]{b/\omega})^{-1}$.

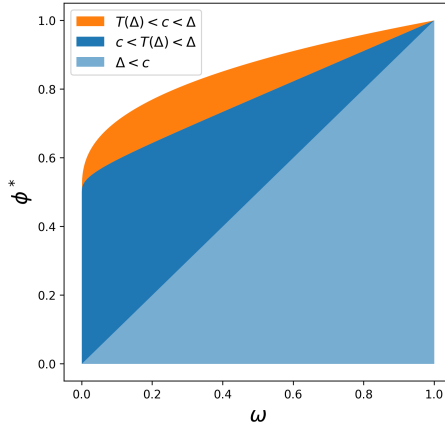


Figure 2: Partition of the parameter space for the unimodal map (9) according to the classification (C1)–(C3).

(A_t) T is topologically transitive on the interval $[T(\Delta), \Delta]$.

In particular, any such T satisfies the dynamical core condition (C3). Notice also that $T(x) > x$ for any $x < T(\Delta)$, in particular, $T'(0) > 1$.

The invariant sets (attractors) of a unimodal map have a variety of structures, as it is stated by the following theorem of Blokh and Lyubich (we quote the statement given in [56, Theorem 6]):

Theorem A ([16]). Let $T : I \rightarrow I$ be an S-unimodal map with nonflat critical point (S means $S(T) < 0$). Then T has a unique metric attractor A , such that the ω -limit set $\omega(x) = A$ for Lebesgue almost all $x \in I$. The attractor A is of one of the following types:

1. an attracting periodic orbit;
2. a Cantor set of measure zero;
3. a finite union of intervals with a dense orbit.

In the first two cases, $A = \omega(c)$.

Associated to T there is the *transfer operator* (also called the *Perron-Frobenius operator*) $L : L^1 \rightarrow L^1$ which is the positive linear operator defined by the duality relation⁶

$$\int_I Lf g = \int_I f g \circ T, \quad f \in L^1, g \in L^\infty.$$

In order to get useful information from this operator, we need to restrict the functional space where it acts; we choose here the Banach space BV of bounded

⁶Without mention of the contrary, all the L^p spaces in the paper will be intended with respect to the Lebesgue measure. The latter will be denoted as dx or Leb .

variation functions on the unit interval equipped with the complete norm

$$\|f\|_{BV} = |f|_{TV} + \|f\|_1,$$

where $|f|_{TV}$ is the total variation of the function $f \in L^1$. For a chaotic map T it follows that it admits a unique absolutely continuous invariant measure $\nu = \nu \circ T^{-1}$ with a density $h \in BV$ and supported on the interval $[T(\Delta), \Delta]$ ([13, Section 5, Corollary 1]). Moreover, ν is mixing with exponential decay of correlations on BV observable, namely there exists $0 < v < 1$ and a constant $C > 0$ such that

$$\left| \int L^n f g dx - \int f dx \int g dx \right| \leq C v^n \|f\|_{BV} \|g\|_\infty, \quad (11)$$

see [13, Section 5, Corollary 3] and [58, Proposition 5.15].

Before continuing, it is useful to quote a sort of analog of the theorem of Blokh and Lyubich given above, for what concerns invariant measures for the map T . We give here the statement of Theorem 9 in [56].

Theorem B (see [45, Chapter V.1]). Let T be an S-unimodal map with nonflat critical point. If T has a periodic attractor, or a Cantor attractor, then T admits a unique SRB measure⁷ supported on the attractor.

If T admits an absolutely continuous invariant probability measure μ , then:

1. μ is a SRB measure;
2. the attractor A of T is an interval attractor;
3. $\text{supp } \mu = A$, in particular, μ is equivalent to the Lebesgue measure on A .

Remark 3.1. As pointed out in [13], (A4) ensures that T has no periodic attractors and is ergodic with respect to the measure μ , which is the unique absolutely continuous invariant probability measure for T . And (A_t) allows to prove that T is Bernoulli and therefore mixing. Therefore chaotic map fulfills conditions 1–3 of Theorem B above. As it is pointed out in [56, Section 4]: “The theorem [above] does not guarantee the existence of a natural measure in the case of an interval attractor. Indeed there are uncountably many parameters in the logistic family, for which the corresponding maps have interval attractors and lack natural measures altogether, or have natural measures with weird properties... But, at least in the logistic family, both such singular phenomena and Cantor attractors are rare in the sense of Lebesgue measure”.

In Section 6 we will address the question to compute the Lyapunov exponent Λ for the map T . The following theorem by G. Keller can be applied to our situation:

⁷We remind that an invariant measure μ is called a Sinai-Ruelle-Bowen (SRB) measure if

$$\mu = \lim_{n \rightarrow \infty} \frac{1}{n} \sum_{k=0}^{n-1} \delta_{T^k(x)}$$

for Leb-a.e. $x \in [0, 1]$, where δ_x is the Dirac mass at x .

Theorem C ([36]). Let $T: I \rightarrow I$ be an S-unimodal map with nonflat critical point. Then T admits an absolutely continuous invariant probability measure if and only if $\lim_{n \rightarrow \infty} \frac{1}{n} \log |DT^n(x)| = \Lambda > 0$, for almost all $x \in I$.

Of course if T has a periodic attractor, the Lyapunov exponent will be negative. The situation is different whenever T has a Cantor attractor. For an S-unimodal map with nondegenerate critical point that also has a Cantor attractor, the Lyapunov exponent will be 0, while there are families of unimodal maps with critical point of sufficiently high order, which have Cantor attractors with sensitive dependence on initial conditions, see [56, Section 5].

3.2 Markov chains

Recall that a Markov chain $\{X_t : t \in \mathbb{N}\}$ on the interval I is given by *transition probabilities*

$$P_x(A) = \mathbb{P}\{X_{t+1} \in A \mid X_t = x\}$$

(the probability that a chain at $x \in I$ will be in a set⁸ $A \subset I$ after one step) and an initial distribution $\rho_0(A) = \mathbb{P}\{X_0 \in A\}$. In the particular case where all P_x , $x \in I$, and ρ_0 are absolutely continuous (with respect to Leb) and are given by densities $p(x, \cdot)$ and h_0 , respectively, we have

$$P_x(A) = \int_A p(x, y) dy, \quad \rho_0(A) = \int_A h_0(y) dy.$$

The map $p: I \times I \rightarrow \mathbb{R}_+$ (known as the *stochastic kernel*) plays the role that the transition matrix does in the theory of Markov chains with a finite state space. For P_x to be a probability, it should satisfy $\int p(x, y) dy = 1$ for every $x \in I$.

Denote with \mathcal{M} the space of (real-valued) Radon measures on I . There is an associated operator $\mathcal{L}: \mathcal{M} \rightarrow \mathcal{M}$ (called the *Markov operator* corresponding to P) acting by

$$\mathcal{L}\rho = \int P_x d\rho(x), \quad \rho \in \mathcal{M}, \tag{12}$$

that is, $\mathcal{L}\rho(A) = \int P_x(A) d\rho(x)$ for every $A \subset I$, or, equivalently,

$$\int \varphi d\mathcal{L}\rho = \iint \varphi(y) dP_x(y) d\rho(x)$$

for all $\varphi \in C^0$, where C^0 denotes the Banach space of continuous functions on I with the sup norm. We note that $\mathcal{L}: L^1 \rightarrow L^1$ is an isometry, where L^1 is intended, from now on, with respect to the Lebesgue measure. If the chain is given by the kernel p , formula (12) restricted to L^1 becomes

$$(\mathcal{L}h)(y) = \int p(x, y) h(x) dx, \quad h \in L^1. \tag{13}$$

⁸All sets considered will be assumed to be measurable. For brevity's sake, we omit the word 'measurable' everywhere in this text.

If ρ_t denotes the distribution of the random variable X_t , then the distribution of X_{t+1} is $\rho_{t+1} = \mathcal{L}\rho_t$. In other words, fixing the distribution ρ_0 for X_0 , the entire sequence of future distributions can be obtained by iterating with \mathcal{L} .

A measure $\mu \in \mathcal{M}_+$ is said to be *stationary* if

$$\mathcal{L}\mu = \mu.$$

Every stationary measure μ gives rise to a shift-invariant measure \mathbb{P}_μ on the sequences space $\Omega = \{(x_t)_{t \in \mathbb{N}} : x_t \in I\}$ of realizations of the process, such that $\mathbb{P}_\mu(x_t \in A) = \mu(A)$ for all $t \in \mathbb{N}$ (see, e.g., [39]). We say that μ is *ergodic* if \mathbb{P}_μ is ergodic. In the next section we will show that, under some mild conditions, our model admits a unique (and thus ergodic) absolutely continuous stationary probability μ with a density $h \in BV$. Then, by the Ergodic Theorem (see, e.g., [15, Remark C4.1]), for every $f \in L^1(\mu)$,

$$\frac{1}{n} \sum_{t=1}^n f(X_t) \xrightarrow[n \rightarrow \infty]{} \int f d\mu, \quad \mathbb{P}_\mu\text{-almost surely.}$$

In particular, realizations of the process are distributed in the state space according to the measure μ .

3.3 Coupling with a stochastic process

We are now ready to define a Markov chain that describes our model. It is obtained as a deterministic unimodal map $T: I \rightarrow I$ satisfying assumptions of Section 3.1, coupled with a stochastic process, namely, by perturbing T with additive noise. Starting from (8) as our main motivation, on the one hand, we consider a more general class and, on the other, impose some mild technical restrictions that are necessary for rigorous analysis.

Since the noise varies in a neighborhood of 0, we will need to extend the state space on the negative axes. We will see in a moment, however, that such an extension is irrelevant for the asymptotic behavior of the perturbed system, whose random trajectories spend all the time, but a relatively short transient, on the positive unit interval.

We fix T and parametrize the chain by the *rebalance time* n (which is roughly inverse to the variance of the noise), consequently indexing with n the chain $(X_t^{(n)})$, the transition probabilities $P_x^{(n)}$ and the stochastic kernel $p_n(x, y)$ where it is necessary. We will be interested in the limit for $n \rightarrow \infty$.

We also need to assume that the noise is compactly supported, in order for trajectories of the process to stay bounded. Compared to the Gaussian noise in (8), this is done by truncating the distribution tails that are exponentially small for large n , see Section 3.4 for the main example.

Denote by

$$\Gamma := 1 - \Delta$$

the gap between $T(c)$ and 1. We now extend the domain of definition of T to the larger interval $[-\Gamma, 1]$ (which, by abuse of notation, will be still denoted

by I) so that T is continuous at 0 and on $[-\Gamma, 0]$ is C^4 smooth, positive and decreasing, with $T(-\Gamma) < \Delta$.⁹

To construct the chain, we need to define transition probabilities. Let $g_{x,n}(y)$ be a probability density supported on a compact interval $[-s(x), s(x)]$. We assume that

- $0 < s(x) < \Gamma/2$ for $x \in (0, 1)$,
- $T(x) - s(x) > 0$ for $x \in (0, 1 - \Gamma/2]$,
- $T(x) - s(x) > x$ for x small (in particular, $T'(0) > 1$).

We set for simplicity $s(x) := 0$ for $x \leq 0$ (meaning $P_x^{(n)} = \delta_{T(x)}$); Lemma 4.4 below shows that this choice does not affect the dynamics. We will also assume that both the mean and the variance of $g_{x,n}$ decrease to 0 as $n \rightarrow \infty$ and, for every $\varepsilon > 0$,

$$\sup_{x \in [\varepsilon, 1-\varepsilon]} |g_{x,n}|_{TV} < \infty. \quad (14)$$

Fix any initial distribution $\rho_0 \in \text{BV}$ and define transition probabilities

$$P_x^{(n)}(A) := \int_{-s(x)}^{s(x)} \mathbb{1}_A(T(x) + y) g_{x,n}(y) dy, \quad (15)$$

which correspond to the stochastic kernel

$$p_n(x, y) = g_{x,n}(y - T(x)). \quad (16)$$

Informally speaking, the probability that the chain steps from x to A will be high whenever $T(x)$ falls in A . Equivalently, we can write

$$X_{t+1}^{(n)} = T(X_t^{(n)}) + Y_{t+1}, \quad \text{where } Y_{t+1} \sim g_{x,n}. \quad (17)$$

The values of $X_{t+1}^{(n)}$ are spread in a neighborhood of $T(x)$ due to the addition of the random variable Y_{t+1} .

3.4 The leverage model

We will slightly modify (8) to satisfy the technical assumptions listed above. The unimodal map is

$$T(x) = \frac{|x(1-x)|}{\sqrt{bx^2 + \omega(1-x)^2}}, \quad (18)$$

⁹A similar extension was considered in [13] to allow perturbations with additive noise; in particular, it was supposed that $T(I) \subset \text{int}(I)$ and that T admits an extension to some compact interval $J \supset I$, preserving all the previous properties and satisfying $T(\partial J) \subset \partial J$. Notice that with this extension the map T is not anymore of class C^4 as prescribed at the beginning of Section 3.1, but this regularity still persist on the interval $(0, 1)$ and this will be enough for the next considerations.

where the parameters ϕ^* and ω are such that T satisfies assumptions (A1)–(A5). (see Section 3.1). It always has negative Schwarzian derivative, as we verified numerically. The condition $T(\Delta) < c < \Delta < 1$ defines a nonempty subset of parameters (see Fig. 2). Notice that $T'(0) = 1/\sqrt{\omega} > 1$.

We want $g_{x,n}$ to be (truncated) normal with a variance close to (10). For this, let us denote by $\mathcal{N}_a(0, \sigma)$ the smoothed truncated normal distribution with the density $g(y) = c_{a,\sigma} \chi_a(y) e^{-\frac{y^2}{2\sigma^2}}$, where $c_{a,\sigma}$ is so that $\int g(y) dy = 1$ and χ_a is a smooth bump function supported on $[-a, a]$.¹⁰ For instance, we may set

$$\chi_a(y) = \begin{cases} 1, & \text{if } |y| \leq (1-\varepsilon)a, \\ \Psi\left(\frac{y \pm (1-\varepsilon)a}{\varepsilon a}\right), & \text{if } (1-\varepsilon)a < |y| \leq a, \\ 0, & \text{if } |y| > a, \end{cases}$$

where $\Psi(t) = e^{1-\frac{1}{1-t^2}}$ is the standard C^∞ bump function on $[-1, 1]$. We set

$$\sigma_n(x) := \frac{bx^3 \sqrt{1-x^2}}{\sqrt{n}(bx^2 + \omega(1-x)^2)^{3/2}}. \quad (19)$$

Denote $\sigma(x) := \sigma_1(x)$ and $\sigma_{\max} := \max_{x \in [0,1]} \sigma(x)$. Set

$$g_{x,n}(y) := c_{x,n} \chi_{s(x)}(y) e^{-\frac{y^2}{2\sigma_n^2(x)}}, \quad (20)$$

where

$$s(x) := \frac{\sigma(x)}{\sigma_{\max}} \min\left\{\frac{\Gamma}{2}, T\left(1 - \frac{\Gamma}{2}\right)\right\} \quad \text{and} \quad c_{x,n} := \left(\int_{-s(x)}^{s(x)} \chi_{s(x)}(y) e^{-\frac{y^2}{2\sigma_n^2(x)}} dy\right)^{-1}.$$

We can then rewrite (17) as

$$X_{t+1}^{(n)} = T(X_t^{(n)}) + \sigma_n(X_t) Z_{t+1}, \quad Z_{t+1} \sim \mathcal{N}_{b_n}(0, 1), \quad (21)$$

with $b_n := \frac{\sqrt{n}}{\sigma_{\max}} \min\left\{\frac{\Gamma}{2}, T\left(1 - \frac{\Gamma}{2}\right)\right\} \rightarrow \infty$ as $n \rightarrow \infty$. The fact that, for n fixed, $g_{x,n}$ are rescaled copies of the same distribution will be used in Section 3.5 to explicitly describe random maps associated to the process. We get the following stochastic kernel:

$$p_n(x, y) = c_{x,n} \chi_{s(x)}(y - T(x)) e^{-\frac{(y-T(x))^2}{2\sigma_n^2(x)}}. \quad (22)$$

Notice also that the support of $p_n(x, y)$ does not depend on n (see Fig. 3).

Finally, (14) holds, because $|g_{x,n}|_{TV} = 2c_{x,n}$ and the latter is proportional to $1/\sigma_n(x)$, which is bounded on $[\varepsilon, 1-\varepsilon]$.

¹⁰The smoothness of the truncation function is only used in the proof of Theorem 6.5.

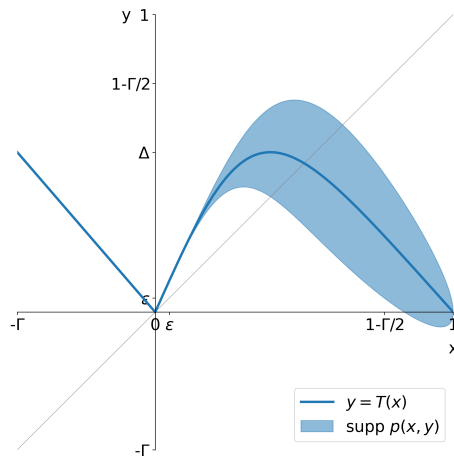


Figure 3: Support of the kernel (22).

3.5 Random transformations

Our model was defined as a Markov chain. We now present a slightly different, yet equivalent, point of view. Namely, we will pick up a family of maps $T_\eta: I \rightarrow I$, $\eta \in [0, 1]$, in such a way that

$$\text{Leb}\{\eta : T_\eta(x) \in A\} = P_x(A) \quad (23)$$

for all $A \subset I$. We can then define a stochastic process

$$\bar{x}_{t+1} = T_{\eta_{t+1}}(\bar{x}_t), \quad (24)$$

where η_t are independent and uniformly distributed in $[0, 1]$. We can write $\bar{x}_t = T_{\eta_t} \circ \dots \circ T_{\eta_1} \bar{x}_0$, where $(\eta_t)_{t \in \mathbb{N}}$ is an i.i.d. stochastic process, i.e. the process (24) follows the orbits under the concatenation of randomly chosen maps from the family. One can show that the two processes are equivalent, see, for instance, [37]. Conversely, starting with a family of maps T_η one can use (23) to define transition probabilities P_x and thus a Markov chain.

Rewriting (23) as $P_x(A) = \int_0^1 \mathbb{1}_A(T_\eta(x)) d\eta$ and plugging into (12) we get the *disintegration formula* for the Markov operator:

$$\mathcal{L} = \int L_\eta d\eta, \quad (25)$$

where L_η are the transfer operators associated with T_η . In particular, a measure μ is stationary for the Markov chain if and only if it satisfies $\mu = \int L_\eta \mu d\eta$, i.e., for all $A \subset I$,

$$\mu(A) = \int \mu(T_\eta^{-1}A) d\eta. \quad (26)$$

Equation (26) is usually taken as the definition of a stationary measure for the family of random maps. Every such measure corresponds to a product measure

that is invariant for the skew-product with the Bernoulli shift in the base and the maps T_η in the fibers; we refer to [4, Section 2] for details.

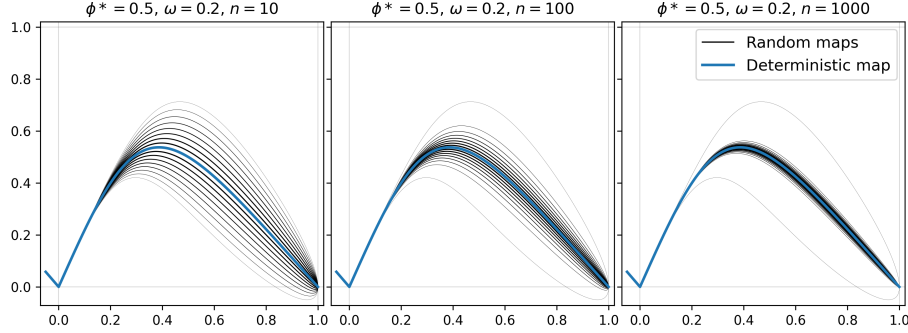


Figure 4: Random maps (27) for $\phi^* = 0.5$, $\omega = 0.2$, $n = 10, 100, 1000$, $\eta = k/16$.

As follows from (21), the random maps for the main example have the form

$$T_\eta(x) = T(x) + q_n(\eta)\sigma_n(x), \quad (27)$$

where q_n is the quantile function of the truncated normal distribution $\mathcal{N}_{b_n}(0, 1)$. Indeed, since q_n maps the uniform measure on $[0, 1]$ to the truncated standard Gaussian measure on $[-b_n, b_n]$, we have

$$\begin{aligned} P_x(A) &= \mathbb{P}\{T(x) + \sigma_n(x)Z_t \in A\} \\ &= \text{Leb}\{\eta : T(x) + \sigma_n(x)q_n(\eta) \in A\} \\ &= \text{Leb}\{\eta : T_\eta(x) \in A\}. \end{aligned}$$

We can equivalently rewrite (27) as

$$T_\eta(x) = T(x) + \tilde{q}_n(\eta)\sigma(x), \quad (28)$$

where \tilde{q}_n is the quantile function of $\mathcal{N}_{b_n}(0, \frac{1}{n})$. Notice that for different n , the set $\{T_\eta\}_{\eta \in [0,1]}$ consists of the same maps, however the ones close to $T = T_{\frac{1}{2}}$ are given bigger weights for large n . More precisely, for every $\delta > 0$, we have

$$\sup_{\eta \in [\delta, 1-\delta]} \sup_{x \in I} |T_\eta(x) - T(x)| \leq \sigma_{\max} \sup_{\eta \in [\delta, 1-\delta]} |\tilde{q}_n(\eta)| \xrightarrow{n \rightarrow \infty} 0. \quad (29)$$

4 Stationary measure

We are now going to establish the existence of a unique stationary measure for the chain. This will be accomplished in the following steps: we first prove the Lasota-Yorke inequality (30); as a consequence we will get a finite number of ergodic absolutely continuous stationary measures whose supports are mutually disjoint up to sets of zero Lebesgue measure. The uniqueness will be proved by showing that all the previous components share a measurable set of positive Lebesgue measure. Throughout this section n is fixed and we will omit it from notations.

4.1 Existence

We will first show that there are *finitely many* ergodic stationary densities of bounded variation. The following lemma will be useful in the sequel.

Lemma 4.1. *For any $\rho \in BV$, if $C := \text{ess sup}_{x \in \text{supp } \rho} |p(x, \cdot)|_{TV} < \infty$, then*

$$|\mathcal{L}\rho|_{TV} \leq C\|\rho\|_1 \quad \text{and} \quad \|\mathcal{L}\rho\|_{BV} \leq (C+1)\|\rho\|_1.$$

Proof. For the first inequality we have

$$\begin{aligned} |\mathcal{L}\rho|_{TV} &= \sup \sum_i \left| \int p(x, y_{i+1})\rho(x)dx - \int p(x, y_i)\rho(x)dx \right| \\ &\leq \sup \sum_i \int |p(x, y_{i+1})\rho(x) - p(x, y_i)\rho(x)| dx \\ &\leq \int |p(x, \cdot)|_{TV} \rho(x) dx \leq C\|\rho\|_1. \end{aligned}$$

The second inequality follows from the first one, since the Markov operator is an isometry, i.e. $\|\mathcal{L}\rho\|_1 = \|\rho\|_1$ for all $\rho \in L^1$. \square

We say that a stochastic kernel $p(x, y)$ has *uniformly bounded variations* if $|p(x, \cdot)|_{TV} \in L^\infty$, i.e. there is $C > 0$ such that $|p(x, \cdot)|_{TV} \leq C$ for almost every $x \in I$.

Proposition 4.2. *If the kernel p has uniformly bounded variations, then the operator \mathcal{L} is quasi-compact and there exist finitely many ergodic stationary measures with densities in BV and, moreover, their supports are mutually disjoint up to sets of zero Lebesgue measure.*

Proof. By Lemma 4.1, for every n ,

$$\|\mathcal{L}^n \rho\|_{BV} = |\mathcal{L}^n \rho|_{TV} + \|\mathcal{L}^n \rho\|_1 \leq C\|\mathcal{L}^{n-1} \rho\|_1 + \|\rho\|_1 = (C+1)\|\rho\|_1.$$

In particular,

$$\|\mathcal{L}\rho\|_{BV} \leq (C+1)\|\rho\|_1 \leq \eta\|\rho\|_{BV} + (C+1)\|\rho\|_1 \quad (30)$$

for any $\eta < 1$. This is the *Lasota-Yorke inequality*. The latter, plus the fact that BV is compactly embedded in L^1 , implies that the peripheral spectrum of \mathcal{L} is discrete and therefore the chain will admit *finitely many* (at least one) absolutely continuous ergodic stationary measures, with supports that are mutually disjoint up to sets of zero Lebesgue measure. Moreover, the essential spectral radius is strictly smaller than the spectral radius (*spectral gap*). These properties, which are consequences of the Ionescu-Tulcea-Marinescu theorem, are summarized by saying that the operator \mathcal{L} acting on BV is *quasi-compact*, see, e.g., [11, 19, 18] for an exhaustive presentation of these results and [10, Section 2.3] for a specific application to random systems. \square

Remark 4.3. Let us mention that whenever the operator \mathcal{L} is quasi-compact and the largest eigenvalue, which is 1 in our case, is simple and therefore there is only one stationary measure with density in BV , then the norm of $\|\mathcal{L}^k f\|_{BV}$ goes exponentially fast to zero when $k \rightarrow \infty$, for $f \in BV$ and $\int f dx = 0$ (exponential decay of correlations). This fact will be extensively used in Section 6.

Since the variance (19) vanishes at 0 and 1, the kernel (22) is in fact unbounded. However, we can still apply Proposition 4.2 under a suitable restriction of the domain of \mathcal{L} . We first state a general result which allows us to confine the stationary measures. For any $\varepsilon > 0$, define the interval

$$I_{\varepsilon, \Gamma} := [\varepsilon, 1 - \Gamma/2].$$

Lemma 4.4. *Under the assumptions of Section 3.3, there is $\varepsilon > 0$ such that any stationary measure μ has $\text{supp } \mu \subset \{0\} \cup I_{\varepsilon, \Gamma}$. If μ is continuous, $\text{supp } \mu \subset I_{\varepsilon, \Gamma}$.*

Proof. First, notice that any stationary measure is supported on the interval $K_\Gamma := [-\Gamma/2, 1 - \Gamma/2]$. Indeed, by invariance, $\mu(K_\Gamma^c) = \int P_x(K_\Gamma^c) d\mu(x) = 0$, because $P_x(K_\Gamma^c) = 0$ for all x .

Fix $\varepsilon > 0$ such that $T(x) - s(x) > x$ for $x \in (0, \varepsilon)$. By choosing a smaller ε if needed, we may also assume that $T(x) - s(x) > \varepsilon$ for $x \in [\varepsilon, 1 - \Gamma/2]$. Then $\inf \text{supp } P_x > \min\{x, \varepsilon\}$ for every $x \in K_\Gamma \setminus \{0\}$. This means that for any realization (x_t) of the process, either all $x_t = 0$ (clearly, 0 is a fixed point, since $P_0 = \delta_0$) or *all but finitely many* $x_t > \varepsilon$.

On the other hand, if $\mu([-\Gamma, \varepsilon] \setminus \{0\}) > 0$, then by the Poincaré recurrence theorem, applied to the shift on (Ω, \mathbb{P}_μ) , \mathbb{P}_μ -almost surely there would exist a realization (x_t) with *infinitely many* $0 \neq x_t < \varepsilon$, which is not possible, as we showed above. This finishes the proof. \square

Theorem 4.5. *The chain defined in Section 3.3 admits finitely many ergodic stationary measures with densities in BV . Moreover, there is $\varepsilon > 0$ such that $\text{supp } \mu \subset I_{\varepsilon, \Gamma}$ for any such measure μ .*

Proof. By Lemma 4.4, the density of any absolutely continuous stationary measure belongs to the subspace $Y := \{h \in L^1 \mid \text{supp } h \subset I_{\varepsilon, \Gamma}\}$. From the first part of the proof of Lemma 4.4 it also follows that Y is \mathcal{L} -invariant. Moreover, the kernel (16) has uniformly bounded variations when restricted to $I_{\varepsilon, \Gamma} \times I_{\varepsilon, \Gamma}$. Indeed, $|p_n(x, \cdot)|_{TV} = |g_{x, n}|_{TV}$ and the latter is bounded on $I_{\varepsilon, \Gamma}$ by (14). We can therefore apply Proposition 4.2. \square

Remark 4.6. It is worth noticing that the preceding result is completely independent of the structure of the unimodal map T . In this respect we could consider maps admitting attracting periodic points or Cantor sets of measure zero, but still producing smooth stationary measures when perturbed with our additive noise.

4.2 Uniqueness

We begin with the following simple lemma that links the topological dynamics of T with the structure of any stationary measure.

Lemma 4.7. *For any stationary measure μ and any open set U , if $\mu(U) = 0$, then also $\mu(T^{-k}U) = 0$ for all $k > 0$.*

Proof. It is enough to show that $\mu(T^{-1}U) = 0$, the result then follows by induction. By invariance we have $0 = \mu(U) = \int P_x(U)d\mu(x) \geq \int_{T^{-1}U} P_x(U)d\mu(x)$. But for every $x \in T^{-1}U$, $T(x) \in U \cap \text{supp } P_x$, and hence $P_x(U) > 0$. Therefore the latter integral can only be zero if $\mu(T^{-1}U) = 0$. \square

With the help of the following lemma we will show that the support of any stationary measure contains the support of the T -invariant measure (atomic in the periodic case). Recall that $x \in \text{supp } \mu$ iff $\mu(U) > 0$ for any open $U \ni x$.

Lemma 4.8. *Let $A \subset I$ be such that (1) T is topologically transitive on A and (2) $\bigcup_{k=0}^{\infty} T^{-k}U = I$ for any open set $U \supset A$. Then $A \subset \text{supp } \mu$ for any stationary measure μ .*

Proof. Given an open set U with $U \cap A \neq \emptyset$, by transitivity $A \subset \bigcup_{k=0}^{\infty} T^{-k}U$, and therefore $\bigcup_{k=0}^{\infty} T^{-k}U = I$. By Lemma 4.7, $\mu(U) > 0$. \square

Now we are ready to state the main result of this section.

Theorem 4.9. *If T is either periodic or chaotic, then the chain defined in Section 3.3 admits a unique stationary measure μ with BV density. Moreover, $\text{supp } \mu$ contains a neighbourhood of the periodic cycle if T is periodic, or the interval $[T(\Delta), \Delta]$ if T is chaotic.*

Proof. If T is periodic, a globally attracting cycle \mathcal{O} satisfies the assumptions of Lemma 4.8, therefore $\mathcal{O} \subset \text{supp } \mu$ for any stationary measure μ . Let us show that $\text{supp } \mu$ contains an open neighbourhood of \mathcal{O} . Recall that $p(x, y) > 0$ if and only if $y \in (T(x) - s(x), T(x) + s(x))$, and T and s are continuous. Given $x_0 \in \mathcal{O}$, let $x_1 \in \mathcal{O}$ be such that $x_0 = T(x_1)$. Since $(x_1, x_0) \in \{(x, y) \mid p(x, y) > 0\}$ and the latter set is open, we can find open sets $U \ni x_1$ and $V \ni x_0$ such that $p(x, y) > 0$ for all $x \in U$, $y \in V$. Also $\mu(U) > 0$, because $x_1 \in \text{supp } \mu$. Denoting h the density of μ , by invariance we get $h(y) \geq \int_U p(x, y)d\mu(x) > 0$ for all $y \in V$, i.e. $V \subset \text{supp } \mu$.

If T is chaotic, then from (A_t) we know that the set $I_\Delta = [T(\Delta), \Delta]$ is invariant for T and that T is topologically transitive when restricted to I_Δ . It also follows from (C3) that $\bigcup_{k=0}^{\infty} T^{-k}I_\Delta = I$, so again we can apply Lemma 4.8.

In both cases, we conclude that $\text{Leb}(\text{supp } \mu_1 \cap \text{supp } \mu_2) > 0$ for any stationary measures μ_1, μ_2 , and therefore by Proposition 4.2 they must coincide. Hence the stationary measure is unique. \square

5 Stochastic stability

Once we consider random perturbations of a deterministic dynamics, an important question is to investigate the stochastic stability of the system, which means to determine if a sequence of stationary measure will converge, in a sense to precise, to the invariant measure of the unperturbed map. In our case the sequence of probability measures is given by $\mu_n := h_n dx$. These measures belong to the set of Borel probability measures on the unit interval, which is a compact metric space with the weak-* topology¹¹. There will be therefore at least one subsequence $(\mu_{n_k})_{k \geq 1}$ converging to a probability measure μ_∞ on I . Our objective is to prove that: (i) μ_∞ is invariant, (ii) it is the same for any convergent subsequence, if more than one, and (iii) it coincides with μ . Whenever that happens we will say that our random system is *weakly stochastic stable*. This result could be strengthened by showing that $\|h_n - h\|_1 \rightarrow 0$, which is called the *strong stochastic stability*; we are not able at the moment to get this result. Instead we now give a *sufficient condition* to get the weak stochastic stability:

(A_q) *There exist $q > 1$ and $C_q > 0$ such that for all $n \geq 1$ we have $\|h_n\|_q \leq C_q$.*

We will see in the next section that with the preceding assumption we can prove the convergence of the Lyapunov exponent (Theorem 6.3) and then verify it numerically, which is an indirect indication of the validity of (A_q).

Lemma 5.1. *For every $x \in I$, $P_x^{(n)}$ converges to δ_{Tx} in the weak-* topology as $n \rightarrow \infty$, i.e. $\int \varphi dP_x^{(n)} \rightarrow \varphi(Tx)$ for all $\varphi \in C^0(I)$.*

Proof. For arbitrary $\varepsilon > 0$ we can split

$$\int \varphi dP_x^{(n)} = \int_{B_\varepsilon(Tx)} \varphi dP_x^{(n)} + \int_{B_\varepsilon(Tx)^c} \varphi dP_x^{(n)}.$$

By Chebyshev's inequality, $P_x^{(n)}(B_\varepsilon(Tx)^c) \leq \text{Var}^2 P_x^{(n)} / \varepsilon^2 \rightarrow 0$ as $n \rightarrow \infty$, while φ is bounded, so the second integral can be made arbitrarily small for n large. Consequently, $P_x^{(n)}(B_\varepsilon(Tx)) \rightarrow 1$, and since φ is continuous, the first integral can be made arbitrarily close to $\varphi(Tx)$. \square

The proof of (i) below follows a suggestion in [5, Theorem D].

Proposition 5.2. *Let μ be a weak-* limit measure of a sequence $\mu_{n_k} = h_{n_k} dx$. If h_{n_k} satisfy (A_q), then*

(i) μ is absolutely continuous with density in L^q ;

(ii) μ is invariant under T .

Proof. (i) Let $\varphi \in C^0(I)$. By Hölder's inequality, with $p = \frac{q}{q-1}$,

$$\left| \int \varphi d\mu \right| = \left| \lim_{k \rightarrow \infty} \int \varphi h_{n_k} dx \right| \leq \lim_{k \rightarrow \infty} \|h_{n_k}\|_q \|\varphi\|_p \leq C_q \|\varphi\|_p.$$

¹¹The weak-* topology is given by the family of seminorms $\|\rho\|_\varphi = \int \varphi d\rho$, $\rho \in \mathcal{M}$, $\varphi \in C^0$.

Therefore the map $L^p \ni \varphi \mapsto \int \varphi d\mu \in \mathbb{R}$ is continuous, since C^0 is dense in L^p , and therefore such a functional will be in L^q , namely $\mu = hdx$, $h \in L^q$, $\|h\|_q \leq C_q$.

(ii) It suffices to prove that any test function $\varphi \in C^0(I)$ satisfies

$$\int \varphi h_{\mathfrak{n}_k} dy - \int \varphi \circ T h_{\mathfrak{n}_k} dy \rightarrow 0.$$

Since $h_{\mathfrak{n}_k} = \mathcal{L}h_{\mathfrak{n}_k} = \int p_{\mathfrak{n}_k}(x, \cdot) h_{\mathfrak{n}_k}(x) dx$, by changing the order of integration in the first integral and subtracting the second, we get

$$\int h_{\mathfrak{n}_k}(x) \left[\int p_{\mathfrak{n}_k}(x, y) \varphi(y) dy - \varphi(T(x)) \right] dx. \quad (31)$$

Since the function $\psi_{\mathfrak{n}_k}(x) := \int p_{\mathfrak{n}_k}(x, y) \varphi(y) dy - \varphi(T(x))$ is uniformly bounded,

$$(31) \leq \|h_{\mathfrak{n}_k}\|_q \|\psi_{\mathfrak{n}_k}\|_p \leq C_q \|\psi_{\mathfrak{n}_k}\|_p.$$

By Lemma 5.1, $\psi_{\mathfrak{n}_k}(x) \rightarrow 0$ for every $x \in I$, and therefore by dominated convergence $\|\psi_{\mathfrak{n}_k}\|_p \rightarrow 0$. \square

Theorem 5.3. *Under Assumption (A_q) , the chain defined in Section 3.3 is weakly stochastic stable, i.e. the stationary probabilities converge to the unique T -invariant probability in the weak- $*$ topology as $\mathfrak{n} \rightarrow \infty$.*

Proof. Since T admits a unique invariant measure, μ must be the same for all convergent subsequences in Proposition 5.2, and therefore the entire sequence $\mu_{\mathfrak{n}}$ converges to μ . \square

It follows from Proposition 5.2 that Assumption (A_q) cannot be satisfied in the periodic case, since the limiting T -invariant measure is singular and supported on the periodic orbit, so Theorem 5.3 only covers the chaotic case. We will now give a proof in the periodic case under the following assumption:

(A_s) *For all \mathfrak{n} sufficiently large and all $x \in \text{supp } \mu_{\mathfrak{n}}$ we have $|T'(x)| \leq \tau < 1$.*

Proposition 5.4. *If T is periodic and satisfies (A_s) , then the chain defined in Section 3.4 is weakly stochastic stable.*

Proof. Let us first consider the case when T has a globally attracting fixed point x_0 . We need to show that for any test function $\varphi \in C^0(I)$ we have $\int \varphi(x) h_{\mathfrak{n}}(x) dx \rightarrow \varphi(x_0)$ as $\mathfrak{n} \rightarrow \infty$. Since $h_{\mathfrak{n}}$ is a fixed point of the random transfer operator (25) and this operator is the dual of the random Koopman operator $\varphi \mapsto \int \varphi \circ T_{\eta} d\eta$ (see, e.g., [4, Section 2] for details), the previous weak limit leads to prove that the following quantity

$$\int_I \int_{[0,1]^k} (\varphi(T_{\eta_k} \circ \dots \circ T_{\eta_1}(x)) - \varphi(x_0)) h_{\mathfrak{n}}(x) d\bar{\eta} dx \quad (32)$$

goes to 0 as $\mathfrak{n} \rightarrow \infty$, where k is an arbitrary fixed number and $\bar{\eta} = (\eta_1, \dots, \eta_k)$.

Given $\varepsilon > 0$, let $\zeta > 0$ be such that $|\varphi(x) - \varphi(x_0)| < \varepsilon$ when $|x - x_0| < \frac{2\zeta}{1-\tau}$. Fix k such that, for all n ,

$$\sup_{x \in \text{supp } \mu_n} |T^k(x) - x_0| < \zeta. \quad (33)$$

Next, fix $\delta > 0$ such that

$$2\|\varphi\|_\infty(1 - (1 - 2\delta)^k) < \varepsilon. \quad (34)$$

Finally, by (29), for all n sufficiently large, we have

$$\sup_{\eta \in [\delta, 1-\delta]} \sup_{x \in I} |T_\eta(x) - T(x)| < \zeta. \quad (35)$$

We now split the integral (32) in the $\bar{\eta}$ variable over the region $E := [\delta, 1 - \delta]^k$ and its complement. On E^c the absolute value of (32) is bounded by (34). Notice that the integral over x takes place on the support of μ_n , where (A_s) holds. Moreover, since the map $[0, 1] \ni \eta \mapsto T_\eta \in C^2(I)$ is continuous, each T_η maps $\text{supp } \mu_n$ to itself; see [6]. Therefore, for $\bar{\eta} \in E$ and $x \in \text{supp } \mu_n$, by (35) and (A_s) , we have

$$|T_{\eta_2} \circ T_{\eta_1}(x) - T^2(x)| \leq |T_{\eta_2}(T_{\eta_1}(x)) - T(T_{\eta_1}(x))| + |T(T_{\eta_1}(x)) - T^2(x)| < \zeta + \tau\zeta.$$

By induction we easily get $|T_{\eta_k} \circ \dots \circ T_{\eta_1}(x) - T^k(x)| < \frac{\zeta}{1-\tau}$ and therefore, in view of (33), $|T_{\eta_k} \circ \dots \circ T_{\eta_1}(x) - x_0| < \frac{2\zeta}{1-\tau}$ for all $\bar{\eta} \in E$ and $x \in \text{supp } \mu_n$. Then, by the choice of ζ , $|\varphi(T_{\eta_k} \circ \dots \circ T_{\eta_1}(x)) - \varphi(x_0)| < \varepsilon$ and the absolute value of (32) over E is therefore bounded by ε .

It is straightforward to modify the above proof for the case when T has a globally attracting periodic orbit of length $m > 1$. One needs to replace T with T^m , the latter will have m attracting fixed points. The corresponding random maps of the form $T_{\bar{\eta}} = T_{\eta_1} \circ \dots \circ T_{\eta_m}$ will be parametrized by $\bar{\eta} = (\eta_1, \dots, \eta_m) \in [0, 1]^m$ endowed with the Lebesgue measure. We leave the details to the reader. \square

Remark 5.5. It follows from the proof that Proposition 5.4 remains valid for the general class of Markov chains defined in Section 3.3 whenever (29) holds, which is in turn the case when T and $g_{x,n}$ are sufficiently smooth.

Remark 5.6. We conjecture that, if T is periodic with the attracting periodic orbit \mathcal{O} , then $h_n \rightarrow 0$ uniformly on compact sets $K \subset I \setminus \mathcal{O}$ as $n \rightarrow \infty$. This property, that we checked numerically, straightens the previous result. In particular,

(A_c) *If T is periodic and the critical point c does not belong to the attracting periodic orbit, then $h_n \rightarrow 0$ uniformly in a neighbourhood of c as $n \rightarrow \infty$.*

6 Lyapunov exponent

6.1 Average Lyapunov exponent

We are interested in the existence of the *Lyapunov exponent* for the slow component, which in our case is defined \mathbb{P}_μ -almost surely as the limit

$$\Lambda = \lim_{n \rightarrow \infty} \frac{1}{n} \sum_{t=0}^{n-1} \log |T'(X_t)| \quad (36)$$

along the chain $(X_t)_{t \geq 0}$. We now motivate such a choice. It is twofold: first of all we want to reproduce the Lyapunov exponent of the unperturbed map T in the limit of zero noise, which we will get in Theorem 6.3; successively we want an indicator which kept memory of the underlying *slow dynamics* played by the map T . We will, in particular, show that such an exponent is negative for periodic T , even in presence of mixing stationary measure.

We now return to (36); if the chain admits a unique stationary probability μ , then, by the ergodic theorem for Markov chains, the above limit equals

$$\int \log |T'| d\mu, \quad (37)$$

assuming $\log |T'| \in L^1(\mu)$.

Remark 6.1. The Lyapunov exponent (37) was called the *average Lyapunov exponent* in [31, 48], and it was associated to the phenomenon of *noise induced order*, which happens when the perturbed systems admit a unique stationary measure depending on some parameter, say θ , and the Lyapunov exponent depends continuously on θ and exhibits a transition from positive to negative values, see also [43] for an experimental evidence of this fact. We will partially prove this phenomenon below by combining Corollary 6.4 and Theorem 6.5, and show it numerically in Section 7.2.

A unimodal map T is said to have a *critical point of order l* if there is a constant D such that $D^{-1}|x - c|^{l-1} \leq |T'(x)| \leq D|x - c|^{l-1}$. In this case it was proved in [49] that the invariant density for T is in L^q , with $q < \frac{l}{l-1}$. We assume in (A3) that T has a critical point of order 2. It is easy to check that (18) satisfies this assumption. Consequently, $\log |T'|$ is in L^p for any $p \geq 1$.

Theorem 6.2. *If T is periodic or chaotic, the limit (36) exists almost surely.*

Proof. The integral (37) is finite, because $\log |T'|$ is in L^1 and the unique stationary measure μ has bounded density, as we proved in Section 4. \square

Once we know that the Lyapunov exponent exists almost surely, it is natural to ask how it depends on the model parameters, for instance, the length m of the fast component series. We have the following

Theorem 6.3. *Suppose one of the following is satisfied: (a) T verifies (A_q) ; (b) T is periodic and verifies (A_s) and (A_c) . Then the Lyapunov exponent (36) converges to the Lyapunov exponent of the deterministic map T as $\mathfrak{n} \rightarrow \infty$.*

Proof. (a) Denote with $\mu_{\mathfrak{n}} = h_{\mathfrak{n}} dx$ the unique stationary measure associated to \mathfrak{n} and with $\mu = h dx$ the unique invariant measure for T . We need to show that

$$\int \log |T'| d\mu_{\mathfrak{n}} \xrightarrow{\mathfrak{n} \rightarrow \infty} \int \log |T'| d\mu. \quad (38)$$

Let $q > 1$ be such that $h_{\mathfrak{n}}, h \in L^q$ and set $p := \frac{q}{q-1}$. Since $\log |T'| \in L^p$, for any $\varepsilon > 0$ there is $\varphi_{\varepsilon} \in C^0$ such that $\|\log |T'| - \varphi_{\varepsilon}\|_p < \varepsilon$. Write

$$\int \log |T'| d\mu_{\mathfrak{n}} = \int (\log |T'| - \varphi_{\varepsilon}) h_{\mathfrak{n}} dx + \int \varphi_{\varepsilon} d\mu_{\mathfrak{n}}$$

and

$$\int \log |T'| d\mu = \int (\log |T'| - \varphi_{\varepsilon}) h dx + \int \varphi_{\varepsilon} d\mu.$$

Since $\log |T'| - \varphi_{\varepsilon} \in L^p$ and $h_{\mathfrak{n}}, h \in L^q$, we have

$$\int |\log |T'| - \varphi_{\varepsilon}| h_{\mathfrak{n}} dx \leq \|\log |T'| - \varphi_{\varepsilon}\|_p \|h_{\mathfrak{n}}\|_q \leq \varepsilon C_q,$$

and the same inequality holds for the integral with respect to μ . Finally, from Theorem 5.3 we know that $\mu_{\mathfrak{n}} \xrightarrow{w^*} \mu$, hence $\int \varphi_{\varepsilon} d\mu_{\mathfrak{n}} \rightarrow \int \varphi_{\varepsilon} d\mu$ as $\mathfrak{n} \rightarrow \infty$.

(b) We know from Proposition 5.4 that $\int \varphi d\mu_{\mathfrak{n}} \rightarrow \frac{1}{|\mathcal{O}|} \sum_{x \in \mathcal{O}} \varphi(x)$ for all $\varphi \in C^0(I)$ as $\mathfrak{n} \rightarrow \infty$, since the T -invariant measure μ is atomic and supported on the attracting periodic orbit \mathcal{O} . Let us first consider the case when the critical point c belongs to \mathcal{O} ; the right-hand side of (38) is then $-\infty$. Denoting $f_m(x) := \max\{\log |T'(x)|, -m\} \in C^0(I)$, for every m we have

$$\int \log |T'| d\mu_{\mathfrak{n}} \leq \int f_m d\mu_{\mathfrak{n}} \xrightarrow{\mathfrak{n} \rightarrow \infty} \frac{1}{|\mathcal{O}|} \sum_{x \in \mathcal{O}} f_m(x) \leq -\frac{m}{|\mathcal{O}|} + C,$$

because $f_m \leq C := \sup \log |T'|$ and $f_m(c) = -m$. Therefore $\int \log |T'| d\mu_{\mathfrak{n}} \rightarrow -\infty$ as $\mathfrak{n} \rightarrow \infty$.

If $c \notin \mathcal{O}$, we can fix a neighbourhood $U \ni c$ given by (A_c) and split

$$\int \log |T'| d\mu_{\mathfrak{n}} = \int_U \log |T'| d\mu_{\mathfrak{n}} + \int_{U^c} \log |T'| d\mu_{\mathfrak{n}}.$$

The first term is bounded by $\|\log |T'|\|_1 \sup_U h_{\mathfrak{n}}$ and vanishes as $\mathfrak{n} \rightarrow \infty$ by (A_c) , while the second one converges to $\int \log |T'| d\mu$ by Proposition 5.4 (approximate $\log |T'| \mathbb{1}_{U^c}$ with a suitable continuous function). \square

Corollary 6.4. *Under the assumptions of Theorem 6.3 and for \mathfrak{n} large enough, Λ is positive if T is chaotic, and negative if T is periodic.*

In a few cases the negativity of the Lyapunov exponent can be shown relatively easily. For instance, denote $\{x \in I \mid |T'(x)| \leq 1\} = [m, M]$ and $\bar{\Delta} := \sup_{x \in I} T(x) + s(x)$. If $T(x) - s(x) > \min\{x, m\}$ for all $x \in (0, \bar{\Delta}]$, then, arguing as in the proof of Lemma 4.4, one can show that any continuous stationary measure μ has $\text{supp } \mu \subset [m, \bar{\Delta}]$. So if, moreover, $\bar{\Delta} \leq M$, then $\Lambda < 0$. Following the classification given in Section 3.1, let us consider the case $T(c) < c$, where the map T exhibits a globally attracting fixed point. In this case, the conditions above will be satisfied if $s(x)$ is small enough, in other words, the stationary measure will be supported in a neighbourhood of the fixed point, where $|T'(x)| \leq 1$. For other cases, we provide some numerical examples in Section 7.2.

6.2 Continuity of the Lyapunov exponent

Denote by $\Theta := \{\theta = (\phi^*, \omega, \mathfrak{n}) \in (0, 1)^2 \times (0, \infty) \mid \max T_\theta < 1\}$ the (extended) parameter space. In order to prove the continuity of the Lyapunov exponent, we will assume that $T_\theta(x) \in C^3(\Theta \times [0, 1])$ and $p_\theta(x, y) \in C^2(\Theta \times (0, 1)^2)$. It is straightforward that our main example defined in Section 3.4 satisfies this assumption. Let $\tilde{\Theta} \subset \Theta$ be the set of parameters θ for which there is a unique stationary measure μ_θ with a density $h_\theta \in BV$; we proved in Section 4 that this is the case if T_θ is periodic or chaotic, but our numerical investigations confirm that in fact $\text{Leb}(\Theta \setminus \tilde{\Theta}) = 0$.

Theorem 6.5. *The mapping $\tilde{\Theta} \ni \theta \mapsto \Lambda_\theta \in \mathbb{R}$ is continuous.*

Proof. Fix an exhaustion of Θ by nested compact sets Θ_ℓ and set $\tilde{\Theta}_\ell := \Theta_\ell \cap \tilde{\Theta}$. It is enough to prove that the mapping $\tilde{\Theta}_\ell \ni \theta \mapsto \Lambda_\theta \in \mathbb{R}$ is continuous on each $\tilde{\Theta}_\ell$, and from now on we fix one of them. As we showed in Lemma 4.4, for each $\theta \in \Theta$, $\text{supp } \mu_\theta \subset I_{\varepsilon_\theta} = [\varepsilon_\theta, 1 - \varepsilon_\theta]$, and since ε_θ can be shown to depend continuously on θ , we can find a single $\varepsilon > 0$ that works for all $\theta \in \Theta_\ell$.

Given $\theta, \theta' \in \tilde{\Theta}_\ell$ we can write

$$\begin{aligned} |\Lambda_\theta - \Lambda_{\theta'}| &= \left| \int \log |T'_\theta| h_\theta dx - \int \log |T'_{\theta'}| h_{\theta'} dx \right| \leq \\ &\int |\log |T'_\theta| | |h_\theta - h_{\theta'}| dx + \int |\log |T'_\theta| - \log |T'_{\theta'}| | h_{\theta'} dx. \end{aligned} \quad (39)$$

To bound the second term in (39), first notice that, by Lemma 4.1,

$$\|h_{\theta'}\|_\infty \leq \|h_{\theta'}\|_{BV} = \|\mathcal{L}_{\theta'} h_{\theta'}\|_{BV} \leq C \|h_{\theta'}\|_1 = C,$$

where

$$C = 1 + \sup_{\theta \in \Theta_\ell} \sup_{x \in I_\varepsilon} |p_\theta(x, \cdot)|_{TV} \leq 1 + \sup_{\theta \in \Theta_\ell} \sup_{x, y \in I_\varepsilon} \left| \frac{\partial p_\theta}{\partial y}(x, y) \right| < \infty$$

is finite, because $\frac{\partial p_\theta}{\partial y}(x, y)$ is continuous and $\Theta_\ell \times I_\varepsilon^2$ is compact. The second term is thus bounded by $C \|\log |T'_\theta| - \log |T'_{\theta'}|\|_1$ and, by Lemma 6.7 below, goes to 0 as $\theta' \rightarrow \theta$.

We now estimate the first term in (39). Since $\log |T'_\theta| \in L^1$, it is enough to bound $\|h_\theta - h_{\theta'}\|_\infty$ which is again dominated by $\|h_\theta - h_{\theta'}\|_{BV}$. By invariance,

$$\|h_\theta - h_{\theta'}\|_{BV} = \|\mathcal{L}_\theta^k h_\theta - \mathcal{L}_{\theta'}^k h_{\theta'}\|_{BV} \leq \|\mathcal{L}_\theta^k (h_\theta - h_{\theta'})\|_{BV} + \|(\mathcal{L}_\theta^k - \mathcal{L}_{\theta'}^k) h_{\theta'}\|_{BV}.$$

As we said in Remark 4.3, the Markov operator \mathcal{L}_θ enjoys the exponential bound

$$\|\mathcal{L}_\theta^k f\|_{BV} \leq C_\theta \zeta_\theta^k \|f\|_{BV}$$

for all $k > 0$ and $f \in BV$ supported on I_ε with $\int f dx = 0$, where the constants $C_\theta > 0$, $0 < \zeta_\theta < 1$ depend on the parameter θ . Since $h_\theta - h_{\theta'}$ has zero mean, we therefore have

$$\|\mathcal{L}_\theta^k (h_\theta - h_{\theta'})\|_{BV} \leq C_\theta \zeta_\theta^k \|h_\theta - h_{\theta'}\|_{BV}.$$

Then

$$(1 - C_\theta \zeta_\theta^k) \|h_\theta - h_{\theta'}\|_{BV} \leq \|(\mathcal{L}_\theta^k - \mathcal{L}_{\theta'}^k) h_{\theta'}\|_{BV},$$

and for k sufficiently large, $C_\theta \zeta_\theta^k < 1$. By a standard trick, expanding a telescopic sum $\mathcal{L}_\theta^k - \mathcal{L}_{\theta'}^k = \sum_{j=1}^k \mathcal{L}_\theta^{k-j} (\mathcal{L}_\theta - \mathcal{L}_{\theta'}) \mathcal{L}_{\theta'}^{j-1}$, we get

$$\begin{aligned} \|(\mathcal{L}_\theta^k - \mathcal{L}_{\theta'}^k) h_{\theta'}\|_{BV} &\leq \sum_{j=1}^k \|\mathcal{L}_\theta^{k-j} (\mathcal{L}_\theta - \mathcal{L}_{\theta'}) h_{\theta'}\|_{BV} \\ &\leq \sum_{j=1}^k C_\theta \zeta_\theta^{k-j} \|(\mathcal{L}_\theta - \mathcal{L}_{\theta'}) h_{\theta'}\|_{BV} \leq C_\theta \frac{1}{1 - \zeta_\theta} \|(\mathcal{L}_\theta - \mathcal{L}_{\theta'}) h_{\theta'}\|_{BV}. \end{aligned}$$

Combining the above inequalities we come to the following estimate:

$$\int |\log |T'_\theta|| |h_\theta - h_{\theta'}| dx \leq M_\theta \|(\mathcal{L}_\theta - \mathcal{L}_{\theta'}) h_{\theta'}\|_{BV},$$

where $M_\theta = \frac{C_\theta \|\log |T'_\theta|\|_1}{(1 - \zeta_\theta)(1 - C_\theta \zeta_\theta^k)}$. It therefore remains to bound $\|(\mathcal{L}_\theta - \mathcal{L}_{\theta'}) h_{\theta'}\|_{BV}$. Since both $h_{\theta'}$ and $(\mathcal{L}_\theta - \mathcal{L}_{\theta'}) h_{\theta'}$ are supported on I_ε and $\|h_{\theta'}\|_\infty \leq C$, we have

$$\|(\mathcal{L}_\theta - \mathcal{L}_{\theta'}) h_{\theta'}\|_1 = \int_{I_\varepsilon} \int_{I_\varepsilon} |p_\theta(x, y) - p_{\theta'}(x, y)| h_{\theta'}(x) dx dy \leq M_1 \|\theta - \theta'\|,$$

where $M_1 = C \sup_{\theta \in \Theta_\iota} \sup_{x, y \in I_\varepsilon} \|\nabla_\theta p_\theta(x, y)\|$ is finite because $\nabla_\theta p_\theta(x, y)$ is continuous and $\Theta_\iota \times I_\varepsilon^2$ is compact. Similarly, arguing as in the proof of Lemma 4.1, we get

$$\|(\mathcal{L}_\theta - \mathcal{L}_{\theta'}) h_{\theta'}\|_{TV} \leq \int_{I_\varepsilon} |p_\theta(x, \cdot) - p_{\theta'}(x, \cdot)|_{TV} h_{\theta'}(x) dx \leq M_2 \|\theta - \theta'\|,$$

with $M_2 = C \sup_{\theta \in \Theta_\iota} \sup_{x, y \in I_\varepsilon} \|\nabla_\theta \frac{\partial p_\theta}{\partial y}(x, y)\| < \infty$. Therefore, the first term in (39) is bounded by $M_\theta (M_1 + M_2) \|\theta - \theta'\|$. This finishes the proof. \square

Remark 6.6. Clearly, the above proof works if we replace $\log |T'|$ with any continuous function. Therefore, the mapping $\tilde{\Theta} \ni \theta \mapsto \mu_\theta \in \mathcal{M}$ is continuous with respect to the weak-* topology on \mathcal{M} , i.e. $\tilde{\Theta} \ni \theta \mapsto \int \varphi \mu_\theta \in \mathbb{R}$ is continuous for any $\varphi \in C^0(I)$. Theorem 6.5 is more delicate, however, because $\log |T'_\theta|$ is neither continuous nor bounded and also depends on θ .

Lemma 6.7. $\|\log |T'_\theta| - \log |T'_{\theta'}|\|_1 \rightarrow 0$ as $\theta' \rightarrow \theta$.

Proof. First notice that the critical point c_θ of the map T_θ depends continuously on the parameter $\theta \in \Theta$. Indeed, since T'_θ is continuous on $\Theta \times I$, the set $\{(\theta, c_\theta)\} = (T'_\theta)^{-1}(\{0\})$ is closed, and then the map $\Theta \ni \theta \mapsto c_\theta \in I$ is continuous by the closed graph theorem.

The functions $\log |T'_\theta|$ and $\log |T'_{\theta'}|$ have logarithmic singularities at c_θ and $c_{\theta'}$ respectively. We will show that these singularities cancel out as $c_{\theta'}$ approaches c_θ . As in the proof of Theorem 6.5, we may assume that $\theta, \theta' \in \Theta_\iota$, where Θ_ι is compact.

Let $\alpha := \sup_{\theta \in \Theta_\iota} |T''_\theta|$. As a direct consequence of the mean value theorem,

$$(|T''_\theta(c_\theta)| - 2\alpha\delta)|x - c_\theta| \leq |T'_\theta(x)| \leq (|T''_\theta(c_\theta)| + 2\alpha\delta)|x - c_\theta|$$

for all $|x - c_\theta| \leq 2\delta$, and the same inequality holds if we replace θ with θ' . Set $D_\delta^\pm := |T''_\theta(c_\theta)| \pm 3\alpha\delta$; both D_δ^+ and D_δ^- are positive, since T_θ has quadratic critical point ($T''_\theta(c_\theta) < 0$). If θ' is sufficiently close to θ , then $|c_\theta - c_{\theta'}| < \delta/2$ and $|T''_\theta(c_\theta) - T''_{\theta'}(c_{\theta'})| < \delta$, and for all $|x - c_\theta| \leq \delta$ we then simultaneously have

$$D_\delta^- |x - c_\theta| \leq |T'_\theta(x)| \leq D_\delta^+ |x - c_\theta|,$$

$$D_\delta^- |x - c_{\theta'}| \leq |T'_{\theta'}(x)| \leq D_\delta^+ |x - c_{\theta'}|,$$

and hence

$$|\log |T'_\theta| - \log |T'_{\theta'}|| \leq \log \frac{D_\delta^+}{D_\delta^-} + \left| \log \frac{|x - c_\theta|}{|x - c_{\theta'}|} \right|.$$

Given $\varepsilon > 0$ and $\theta \in \Theta_\iota$, we first fix $\delta > 0$ such that $\log \frac{D_\delta^+}{D_\delta^-} < \frac{\varepsilon}{3}$ and then let $\theta' \rightarrow \theta$. The integral of the second term is elementary and vanishes as $c_{\theta'} \rightarrow c_\theta$, so $\int_{B_\delta(c_\theta)} \left| \log \frac{|x - c_\theta|}{|x - c_{\theta'}|} \right| dx < \frac{\varepsilon}{3}$, provided θ' and θ are sufficiently close, and

$$\int_{B_\delta(c_\theta)} |\log |T'_\theta| - \log |T'_{\theta'}|| dx < \frac{2\varepsilon}{3}. \quad (40)$$

Let us show that $\log |T'_\theta| - \log |T'_{\theta'}| \rightarrow 0$ uniformly on $B_\delta(c_\theta)^c$. Denote $\beta := \inf_{x \in B_\delta(c_\theta)^c} |T'_\theta(x)| > 0$. We have $\|T'_\theta - T'_{\theta'}\|_\infty \leq M\|\theta - \theta'\|$, where $M = \sup_{\theta \in \Theta_\iota, x \in I} \|\nabla_\theta T'_\theta(x)\|$. Therefore $\inf_{x \in B_\delta(c_\theta)^c} |T'_{\theta'}(x)| > \frac{\beta}{2}$ if $\|\theta - \theta'\| < \frac{\beta}{2M}$. Consequently, $|\log |T'_\theta| - \log |T'_{\theta'}|| < \frac{2M}{\beta}\|\theta - \theta'\|$, and for $\|\theta - \theta'\| < \frac{\varepsilon\beta}{6M}$ we have

$$\int_{B_\delta(c_\theta)^c} |\log |T'_\theta| - \log |T'_{\theta'}|| dx < \frac{\varepsilon}{3}. \quad (41)$$

Combining (41) with (40) we finally get $\|\log |T'_\theta| - \log |T'_{\theta'}|\|_1 < \varepsilon$. \square

6.3 Random Lyapunov exponent and random entropy

In (36) we used the derivative of the deterministic map only. Alternatively, if we define the process using the random transformations (24), we are led to compute the Lyapunov exponent of the cocycle given by the derivative computed along the random orbit, namely we define the *random Lyapunov exponent* (RLE) $\bar{\Lambda}$ as

$$\bar{\Lambda} := \lim_{n \rightarrow \infty} \frac{1}{n} \log |D(T_{\eta_n} \circ \cdots \circ T_{\eta_1})(x)|, \quad (42)$$

for almost every sequence $(\eta_k) \in [0, 1]^{\mathbb{N}}$ with respect to the measure $\text{Leb}^{\otimes \mathbb{N}}$ (see Section 3.5), and almost every $x \in I$ with respect to the stationary measure μ_n . By using the notation introduced in Section 3.5: $\bar{x}_k(x) := T_{\eta_k} \circ \cdots \circ T_{\eta_1}(x)$, with $\bar{x}_0(x) = x$, formula (42) is equal to

$$\bar{\Lambda} = \lim_{n \rightarrow \infty} \frac{1}{n} \sum_{k=1}^n \log |T'_{\eta_k}(\bar{x}_{k-1})|, \quad (43)$$

again for $\text{Leb}^{\otimes \mathbb{N}}$ -a.e. $(\eta_k) \in [0, 1]^{\mathbb{N}}$ and μ_n -a.e. $x \in I$. By using the ergodic theorem for random transformations, see [37] or [7, Section 3.1], we have that

$$\bar{\Lambda} = \int \log |T'_{\eta}(x)| d\mu_n(x) d\eta.$$

Notice that if we compare this random exponent with Λ , we see that the difference between the two is bounded by

$$|\Lambda - \bar{\Lambda}| \leq \int |\log |T'_{\eta}(x)| - \log |T'(x)|| d\mu_n(x) d\eta.$$

By using expression (28) for T_{η} , we can bound the error term in a more explicit way as

$$|\Lambda - \bar{\Lambda}| \leq \int \left| \log \left| 1 + \frac{\tilde{q}_n(\eta) \sigma'(x)}{T'(x)} \right| \right| h_n(x) dx d\eta.$$

Since σ' is bounded over $I_{\varepsilon, \Gamma}$, $\log |T'| \in L^p, p \geq 1$, and finally $\|h_n\|_q \leq C_q$ for all n , we have

$$|\Lambda - \bar{\Lambda}| \leq C_q \int \left\| \log \left| 1 + \frac{\tilde{q}_n(\eta) \sigma'}{T'} \right| \right\|_p d\eta.$$

We expect that this error converges to zero for large n , since the quantile function converge to zero almost everywhere. Table 1 in Section 7.2 shows that, in fact, the error remains very small even for small values of n .

It is known that whenever the random Lyapunov exponent (42) is positive, then it equals the *random entropy*, which is the random generalization of the Kolmogorov-Sinai entropy: this equality is called the *entropy formula*. Roughly speaking, the random entropy computes the limit of the Shannon entropy of the join partition generated by the successive application of the backward images of the random maps on an initial generating partition, aka the entropy rate.

We defer to [37, Theorem 1.3] for the precise definition and [7, Theorem 3.2] for the connection with the RLE. What is important for us is that the random entropy coincides with the much easier object which is the RLE when the latter is positive.

In Corollary 6.4 we proved that the Lyapunov exponent (36) may be negative, and there is strong numerical evidence that the RLE (43) is also negative for certain parameters; see Section 7.2. By assuming that the RLE is negative or zero, we then get that the random entropy is also zero, by using another important result connecting entropy and Lyapunov exponents, namely the Margulis-Ruelle inequality (see for instance [54]), which states that the metric entropy is bounded by the maximum between zero and the sum of the positive Lyapunov exponents. The random version of this inequality, which we use, has been proved by Kifer in [37, Theorem 1.4].

We should now stress the interesting fact that although the entropy is zero, the Markov chain *mixes exponentially fast*, as we pointed out in Remark 4.3. This means that for any observables $f \in L^1$, $g \in BV$ the correlations $\int (\mathcal{L}_n^k f)(x)g(x)dx$ converge to $\int f(x)d\mu_n(x) \int g(x)dx$ exponentially fast when $k \rightarrow \infty$. This result can be stated in a more suggestive way by relying on random transformations. By using the notations introduced in Section 3.5, we can in fact rewrite the previous correlation in terms of composition of randomly chosen maps and say that there exist $0 < v < 1$ and $C > 0$, depending only on the system, such that, for all $k \geq 0$,

$$\left| \iint f(x)g(T_{\eta_k} \circ \dots \circ T_{\eta_1}(x))d\bar{\eta}dx - \int f d\mu_n \int g(x)dx \right| \leq Cv^k \|f\|_1 \|g\|_{BV}.$$

This exponential decay of correlations is a consequence of the spectral gap prescribed by the quasi-compactness of the Markov operator proved in Proposition 4.2, and of the uniqueness of the absolutely continuous stationary measure, see [10] for details; of course these properties hold even when the Lyapunov exponent is negative or zero.

7 Numerical results

In this section we describe and discuss some numerical experiments in support of our rigorous theoretical investigations. Specifically, we present the bifurcation diagram associated with the unimodal map (18) and compute the corresponding Lyapunov exponents for both the deterministic and the stochastic version of the map, see Subsections 7.1 and 7.2, respectively.¹²

7.1 Bifurcation diagram

In this subsection we analyse the dynamics of the unimodal map (18). The bifurcation diagram of a dynamical system shows how the asymptotic distribu-

¹²The code to reproduce all the figures and tables of this section are available from the corresponding author upon reasonable request.

tion of a typical orbit varies as a function of a parameter. For our map either the memory parameter ω or the parameter ϕ^* can be employed as bifurcation parameter. Fig. 5 shows the bifurcation diagram as a function of ϕ^* (the bifurcation diagram as a function of ω looks similar). The choice of the parameters for this plot corresponds to a vertical segment in the parameter space (see Fig. 2) with $\omega = 0.5$ and ϕ^* varying in a neighbourhood of the dynamical core area. As explained in Section 3.1, Theorem A, the invariant set of the unimodal map (18) could be an attracting periodic orbit, a Cantor set of measure zero or a finite union of intervals with a dense orbit, depending on the parameters ω and ϕ^* . Specifically, there is an attracting fixed point or a 2-cycle outside the dynamical core region, whereas in the dynamical core the situation is more complex as small parameter variations can change the dynamics from chaotic to periodic and back, as we see in Fig. 5. To identify more precisely the signature of a chaotic behaviour, in the next subsection we compute the Lyapunov exponent as a function of ϕ^* .

7.2 Lyapunov exponent

The Lyapunov exponent for the deterministic map (18) is positive if and only if T admits an absolutely continuous invariant measure, see Theorem C in Section 3.1. Fig. 6 shows the estimated Lyapunov exponent in the same slice of the parameter space as in Fig. 5. Notice that the exponent becomes a smooth function of ϕ^* when we add even a very small noise, in agreement with the results of Section 6.2. Fig. 7 shows the contour plot of the Lyapunov exponent as a function of ϕ^* and ω both for the deterministic map (18) and for the stochastic process described in Section 3.4. The right panel shows a clear noise-induced regularization phenomenon. In fact, for the stochastic version of the map the intricate fine structure in the parameter dependence of the Lyapunov exponent disappears and is replaced by a smooth dependence.

To provide a numerical exemplification of the stochastic stability and of Theorem 6.3, we computed average (36) and random (43) Lyapunov exponents, as well as the Lyapunov exponent for the deterministic map (18), for different values of ϕ^* , ω and n . The results are presented in Table 1. Within each row, the two subrows are ALE and RLE, respectively: the two agree very well, in most cases up to the precision of the numerical computation. In both cases we sampled 128 independent realizations of the process, each of length 10,000.

8 Estimating the map parameters via deep neural networks

We now consider the problem of estimating the parameters of the map from (short) time series. This is motivated by the fact that in Section 9 we empirically investigate a dataset of US commercial banks leverage. We will consider the time series of bank's leverage as realizations of the process described in Section 3.4

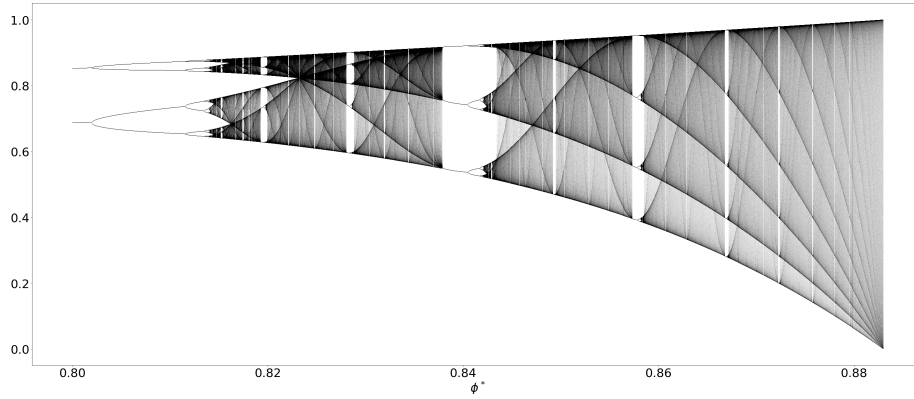


Figure 5: Bifurcation diagram for T in the dynamical core region ($\omega = 0.5$).

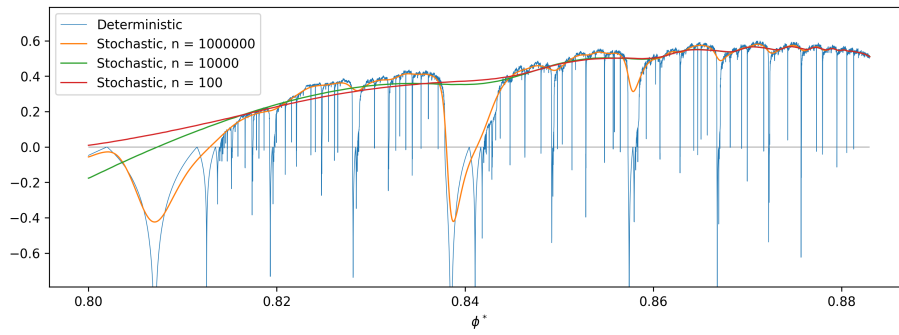


Figure 6: Lyapunov exponents for deterministic and stochastic maps ($\omega = 0.5$).

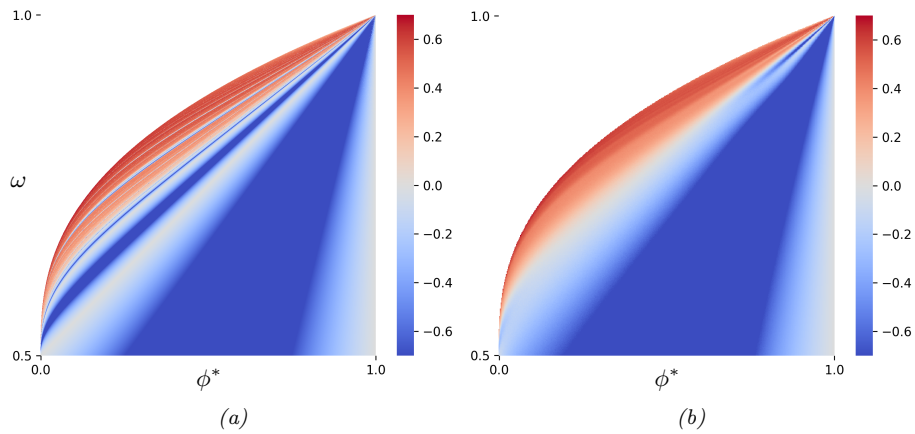


Figure 7: Contour plot of the average Lyapunov exponents for (a) deterministic and (b) stochastic maps ($\bar{n} = 1$).

ϕ^*	ω	DC	Per.	Lyapunov exponent				
				n				Det.
				1	10^3	10^6	10^9	
0.845	0.557	yes	no	0.287	0.287	0.349	0.341	0.340
				0.286	0.286	0.349	0.341	
0.795	0.390	yes	no	0.345	0.346	0.389	0.398	0.400
				0.345	0.346	0.389	0.399	
0.904	0.627	yes	no	0.557	0.557	0.560	0.550	0.552
				0.558	0.557	0.560	0.550	
0.821	0.439	yes	yes	0.378	0.375	-0.051	-0.159	-0.158
				0.378	0.375	-0.052	-0.159	
0.944	0.826	yes	yes	0.296	0.297	0.049	-0.123	-0.122
				0.297	0.296	0.052	-0.123	
0.766	0.323	yes	yes	0.320	0.324	0.286	-0.076	-0.046
				0.320	0.325	0.286	-0.076	
0.258	0.837	no	yes	-0.243	-0.248	-0.248	-0.248	-0.248
				-0.286	-0.248	-0.248	-0.248	
0.908	0.804	no	yes	-0.284	-0.285	-0.365	-0.362	-0.362
				-0.286	-0.287	-0.366	-0.362	
0.541	0.227	no	yes	-0.619	-0.441	-0.380	-0.380	-0.380
				-0.578	-0.446	-0.380	-0.380	

Table 1: Average and random Lyapunov exponents for different values of n compared to the Lyapunov exponent for the deterministic map. DC stands for dynamical core, Per. for periodic, and Det. for the Lyapunov exponent of the deterministic map.

and will estimate for each bank the model parameters. Each time series is very short, being composed by only 59 points.

Given the random nature of the map, one could use maximum likelihood estimation to estimate the parameters. However, this approach is not feasible for two reasons. First, the likelihood function is highly non-convex, so that standard optimization methods may perform poorly. Second, although the likelihood function for the process itself can be written explicitly, in many cases it may happen that the observed time series are systematically undersampled and this prevents an explicit calculation of the likelihood function. For example, we may observe only one slow time scale, corresponding to portfolio rebalancing, out of two, or even out of three (i.e. the bank's risk assessment and portfolio composition may be updated more frequently than our quarterly observations, for instance at a monthly frequency). If we observe, for instance, only the second iterate of the process,

$$\phi_{t+2} = T(T(\phi_t; \theta); \theta) + \sigma(\phi_t; \theta)\epsilon_t + \sigma(\phi_{t+1}; \theta)\epsilon_{t+1}, \quad t \in \mathbb{Z},$$

the transition probabilities $p(\phi_{t+2}|\phi_t; \theta)$, $t \in \mathbb{Z}$, are no longer Gaussian (as it would be the case if we observe the first iterate). Hence, there is apparently no effective formula for the likelihood function.

For this reason, to estimate the parameters of the map, we propose to use a convolutional neural network (CNN) consisting of a sequence of convolutional layers followed by a sequence of dense, or fully connected, layers; we refer to [33, Chapter 9] for detailed exposition of CNNs. In order to deal with the possibility that the observed time-series are realizations of certain iterates of the process, we separately optimize two CNN architectures to be used sequentially. First, we optimize a CNN (henceforth denoted by CNN1) for estimating the number of iterates between observations: it takes as input time series of length 59 and outputs the corresponding value k of the map’s iterate that generated the time-series. Second, for each value of k , we optimize a CNN (henceforth denoted by CNN2(k)), having the exact same inputs, to output the corresponding parameters (ϕ^*, ω) that generated the time-series. Once the parameters (ϕ^*, ω) are estimated, the variance of the noise (and therefore \mathfrak{n}) can be estimated by standard methods. To train CNN1 and CNN2(k) we used a training set of one million samples simulated from the model in Section 3.4 with values of the parameters $\theta = (\phi^*, \omega, \mathfrak{n})$ which uniformly span the parameter space. For both steps, when simulating the series, the initial state of the system was taken randomly from a uniform distribution on $[0, 1]$. This is especially important because of the relatively short length of the series at hand. Therefore, being based only on simulations, the NN approach, contrary to the maximum likelihood one, can work also for partial observations.

The architectures of CNN1 and CNN2(k) are schematized in Fig. 8. In general, a convolutional layer is composed of n_f filters and each filter is associated with one kernel that is applied to a small moving window of the time-series; for instance, in our first convolutional layer $n_f = 128$ and all the windows are of width 2. The outputs of one convolutional layer are connected to the next layer. The weights of these connections constitute the NN parameters to be optimized. After seven convolutions, the output is passed to a sequence of dense layers, which concludes the NN. We use the rectified linear unit (ReLU) function as activation function. Now, we describe the experimental setup.

The implementation is carried out in Python. To generate training and testing data we simulate one million samples. CNN1 is optimized with the stochastic gradient descent method by using the Adam algorithm [38], the categorical cross-entropy as loss function, and the accuracy as metric, with L^2 regularization of weights. Instead, to optimize CNN2 we use the Mean Squared Error (MSE) both as loss function and as metric. The batch size is 32 in both cases. The seven convolutional and three dense layers have a total of 74,818 trainable parameters.

The CNN models show a good performance. We tested our methods on a testing set of 100,000 out of sample time series. Fig. 9 shows the accuracy of CNN1 to estimate the iterates on test data. We choose $k = 1, 2, 3$ because of our empirical application of Section 9. The MSE of CNN2(k) on the test set is about 0.001 for each k . Since both ϕ^* and ω are uniformly distributed in $[0, 1]$, the MSE is quite small and the NN effective.

```

Model CNN1: "convolutional_categorical_model"
-----
Layer (type)                Output Shape                Param #
-----
reshape (Reshape)           (None, 59, 1)              0
conv1d_1 (Conv1D)           (None, 58, 128)           384
conv1d_2 (Conv1D)           (None, 29, 64)            16448
conv1d_3 (Conv1D)           (None, 15, 64)            8256
conv1d_4 (Conv1D)           (None, 8, 64)             8256
conv1d_5 (Conv1D)           (None, 4, 64)             8256
conv1d_6 (Conv1D)           (None, 2, 64)             8256
conv1d_7 (Conv1D)           (None, 1, 64)             8256
flatten (Flatten)           (None, 64)                 0
dense_1 (Dense)             (None, 128)                8320
dense_2 (Dense)             (None, 64)                 8256
dense_3 (Dense)             (None, 3)                  195
=====
Trainable params: 74,883

Model CNN2: "convolutional_model"
...
-----
dense_3 (Dense)             (None, 2)                  130
=====
Trainable params: 74,818

```

Figure 8: Architectures of the CNN1 model used to estimate the iterate k and the CNN2(k) model used to estimate the parameters (ϕ^*, ω) for each k . The two models differ only in the output layer.

9 Chaos in real bank leverage time series

In this section we perform an empirical analysis of a large set of bank's leverage time series. We first describe the data set. Next, through CNN1 and CNN2(k), we estimate the observed iterate k as well as the parameters (ϕ^*, ω) of the model and discuss the results, investigating the relation between the estimated parameters and the bank's size. Finally, to perform an independent analysis supporting our conclusion, we apply the Chaos Decision Tree Algorithm [57] to these time-series and compare the resulting classification with the one obtained with NN estimates.

9.1 Data set

We use the data set of US *Commercial Banks and Savings and Loans Associations* provided by the *Federal Financial Institutions Examination Council* (FFIEC). For the sake of completeness, we provide here a description of it, referring to [28] and references therein for further details. A Commercial Bank

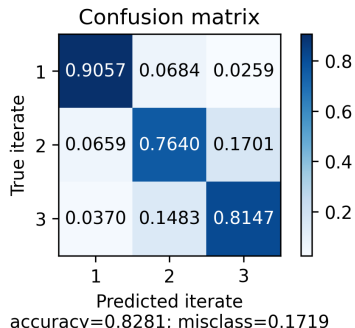


Figure 9: Accuracy of the CNN1 model used to estimate the iterates.

is defined¹³ officially by the FFIEC as: “[...] a financial institution that is owned by stockholders, operates for a profit, and engages in various lending activities”. Commercial banks quarterly fill the *Consolidated Report of Condition and Income* (generally referred to as *Call Report*) as required by the FFIEC. A Savings and Loan Associations, instead, is a financial institution that accepts deposits primarily from individuals and channels its funds primarily into residential mortgage loans. Starting from the first quarter of 2012 they are required to file the same reports of Commercial Banks, thus they are included in the data set since then. The data provided by the *Call reports* are publicly available since 1986 although the level of details required has increased over time. To have a good compromise between the fine structure of data and a reasonably populated statistics we follow [28] and consider the time period going from March 2001 to December 2014, for a total of 59 quarters. Also we consider only the financial institutions that are present in the data set in all the quarters for a total of 5,031 banks. The financial leverage λ_t of each institution at time t is defined as the ratio between the sum of its assets and its equity at time t . In particular, the latter is given by $E_t = A_t - L_t$ where L_t represents the liabilities and A_t the assets of the bank, thus $\lambda_t = A_t/E_t$.

9.2 Estimation via neural networks

In order to estimate the parameters of the map on the just-described data set, we need to fix the value of the liquidity parameter γ ; remind that we consider the linear transformation $\phi_t = (\lambda_t - 1)/\gamma$. In this work, we assume that the liquidity parameter γ of the risk investment is the same for all the banks in our data set. Admittedly, this is a simplifying assumption, coherent with the so-called assumption of statistical equivalence for risky investments (see also [44]), which allows for an analytical tractability of the model; a complete exploration of a relaxation of this hypothesis is beyond the scopes of the present paper and is, therefore, left for future work. In order to fix its value, we exclude 662 time

¹³See <http://www.ffiec.gov/nicSearch/FAQ/Glossary.html>.

series (out of 5,031) that contain outliers, which we define to be values that are two standard deviations away from the mean. We then set γ to the maximum over the remaining 4,369 series, obtaining $\gamma = 15.969$.

Since the time series that we analyze contain quarterly data and portfolio decisions may be made more frequently, it is natural to assume that the observed time series are realizations of certain iterates of the process; we assume $k \in \{1, 2, 3\}$. Fig. 10a displays the output of CNN1. It turns out that only a small percentage (about 1%) of the banks in our data set rebalance their portfolios at a quarterly frequency. Most banks seem to rebalance either every six weeks ($k = 2$, about 55%) or every month ($k = 3$, about 43%). One may ask if the portfolio re-balancing frequency is related to the size of the bank (defined as the average across the 59 quarters of the sum of the dollar-amount of all the type of assets detained by it), for example because larger banks manage more actively their portfolio. Fig. 10b shows the box plots of the logarithm of the size of the banks for $k = 1, 2, 3$. We observe that there is not a statistically significant difference among them.

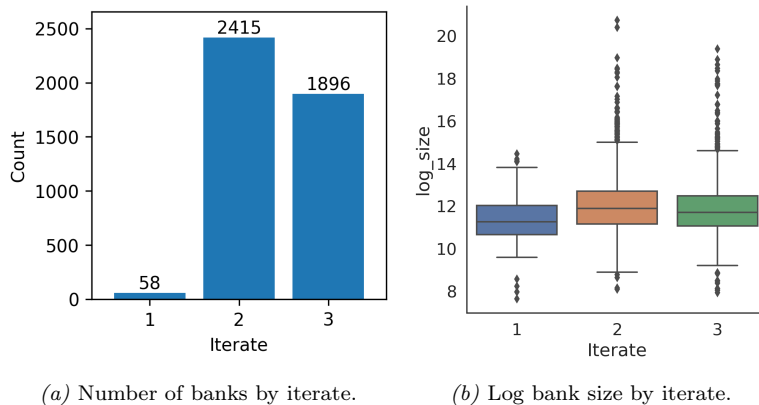


Figure 10: Results on the iterate of the process.

Once the number of iterates k has been identified, we proceed to the study of the chaotic behaviour of the time series. We divide the banks in the three groups identified by k and employ CNN2(k) in order to estimate the parameters (ϕ^*, ω) . In Fig. 11a we plot the estimates of ϕ^* against those of ω ; pairs belonging to the dynamical core region are displayed in red, whereas those falling outside the dynamical core region are displayed in blue. Interestingly, the percentage of banks for which the estimates (ϕ^*, ω) are in the dynamical core region is about 12%. Moreover, Fig. 11b indicates that k is very often equal to two for these banks.

We now ask if bank size is related with the fact that the estimated pair (ϕ^*, ω) is or not in the dynamical core region. Fig. 12a shows the probability density functions of the logarithm of the banks size, by considering separately banks inside and outside the dynamical core, and Fig. 12b displays the corresponding

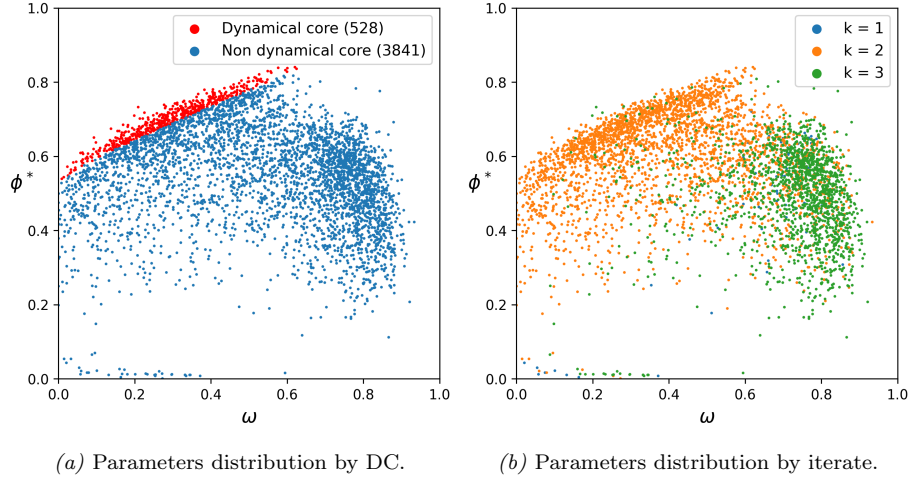


Figure 11: Estimated parameters for iterates in $\{1, 2, 3\}$.

probability-probability plot. To test that the difference between the distribution of banks sizes in and outside the dynamical core region is statistically significant we perform the Kolmogorov-Smirnov test of the null hypothesis that the two samples have the same distribution. The statistics of the test is 9.31×10^{-2} corresponding to a p -value of 5.9×10^{-4} . This latter value shows that the two subsamples have different distributions.

Summarizing, we have found that the parameters of a sizable fraction of banks lie in the dynamical core region and that the dynamics of the leverage of the larger banks tends to be more frequently in the dynamical core than that of the smaller banks.

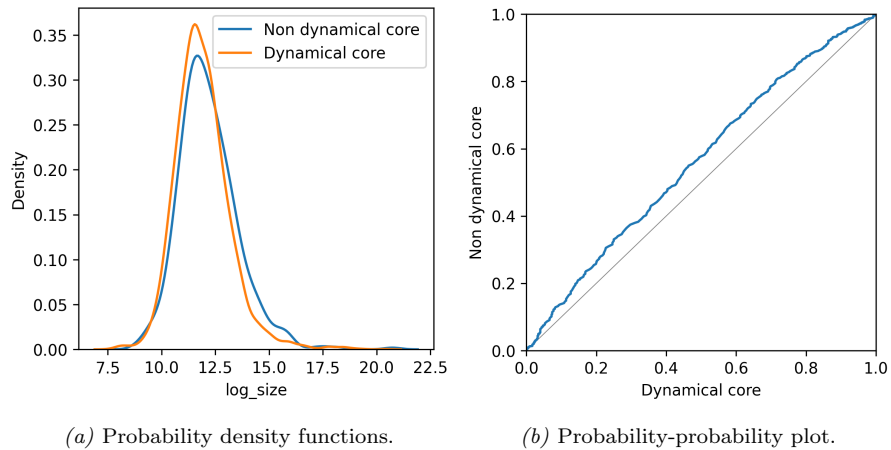


Figure 12: Results on the parameters of the process and bank size.

9.3 Classification via the Chaos Decision Tree Algorithm

Finally, we perform an independent analysis on the bank’s leverage time series by making use of the recently proposed Chaos Decision Tree Algorithm (CDTA) [57], described in detail in Appendix A. This is a non-parametric method which classifies an input time series as chaotic, periodic, or stochastic¹⁴. We perform this analysis for two reasons. First, we know that chaotic behavior can be present only for series generated by our map with parameters in the dynamical core. Thus we test whether the series classified as chaotic by CDTA have estimated parameters in the dynamical core. The second reason is to count how many banks in the dynamical core are identified as chaotic or periodic by CDTA. The Appendix also contains the results of the application of CDTA to data simulated by our map for different time series length, level of noise \mathfrak{n} , and number of iterates k .

Applying CDTA, we find that 64% of the banks are classified as stochastic, $\sim 12\%$ as periodic and $\sim 23\%$ as chaotic. The consistency between the classification made by CDTA and the partition ‘dynamical core’ and ‘not dynamical core’ of the parameters space (ϕ^*, ω) found by the NN model can be assessed by looking at Table 2. We find that a large fraction of series outside the dynamical core are classified as stochastic by CDTA, while a third of banks in the dynamical core is classified as chaotic. This fraction is significantly smaller for banks outside the dynamical core. Thus, despite the agreement is not perfect, we find a reasonable consistency between the conclusions of the two methods and, more importantly, find significant (and independent) support to the conclusion that a sizable fraction of bank time series are described by a chaotic dynamics.

	Periodic	Chaotic	Stochastic
Non dynamical core	382 (9.98%)	648 (16.93%)	2798 (73.09%)
Dynamical core	107 (20.34%)	176 (33.46%)	243 (46.20%)

Table 2: Number of banks by classes.

Finally, the findings reported in the previous subsection suggest a positive relation between the size of a bank and the probability that the dynamics of the (corresponding) leverage time series is chaotic. To verify this observation by using the CDTA classification, we first rank the banks in quintiles according to their size and within each quintiles we compute the percentage of banks that are detected to be stochastic, periodic and chaotic. Table 3 collects the results. In a nutshell, banks having a larger size have, on average, a larger percentage of leverage time series detected as chaotic. A χ^2 -test applied to contiguous quintiles rejects the hypothesis of independence of the CDTA classification from the quintile, indicating that the difference in frequencies across quintiles are statistically significant. Thus also the CDTA analysis confirms that larger banks are more likely characterized by chaotic time series of leverage.

¹⁴Notice that the definitions of *chaotic* and *periodic* for the CDTA differ from the ones given in Section 3.1, see Appendix A.

Statistics	q ₁	q ₂	q ₃	q ₄	q ₅
Chaotic (%)	18.2	20.2	21.7	23.6	29.1
Periodic (%)	12.9	11.6	12.9	13	11.8
Stochastic (%)	68.6	67.3	65	63	58.9

Table 3: Fraction of banks classified as chaotic, periodic, or stochastic by CDTA conditionally to the decile of the bank size.

10 Conclusions

Most risk management practices (as, for example, Value-at-Risk) assume that prices are not affected by actions of other financial institutions that are managing the risk of their portfolio. In other words, these practices assume that risk is exogenous. In reality, in the presence of limited liquidity, coordinated and homogeneous risk management can create market instability and result in what is known as endogenous risk. This has the potential to amplify market instabilities and create crashes through the well-known feedback between leverage, risk, and asset prices. An additional, and less considered, feedback between past and future risks is present because financial institutions use historical data to estimate both the riskiness of their investments and their correlations. This creates new threats for the systemic stability of financial markets. Studying how these two feedbacks affect the leverage dynamics is of paramount importance for understanding systemic risk.

In this paper we consider a stylized model where both feedbacks are present. We showed that the dynamics of the bank’s leverage is described by a unimodal map on $[0, 1]$ perturbed with additive and heteroscedastic noise. The perturbed system can be described in two equivalent ways as a stationary Markov chain or in terms of random transformations. In both cases a fundamental object is the *stationary measure* of the process which allow us to properly define and state all the statistical properties of the system. We are able to construct such a measure and to prove its uniqueness. Moreover we show, under a few assumptions, the stochastic stability of the perturbed system, namely the weak convergence of the stationary measure to the invariant measure for the unimodal map in the zero noise limit. We also define an average Lyapunov exponent, still in terms of the stationary measure, as a sensible indicator of the slow motion, and prove its continuity with respect to the parameters defining the system. We show that, depending on the parameters, the average Lyapunov exponent can be either negative or positive, leading to two qualitatively different (periodic- and chaotic-like) dynamics of the leverage.

We then estimate the parameters of the map via a method based on deep neural networks, whose efficiency was tested in a large testing set. Assuming the proposed unimodal map with heteroscedastic noise as data generating process for the banks leverage, we estimated the parameters on quarterly data of about 5,000 US Commercial Banks via the proposed CNN architecture. By investigating the period from March 2001 to December 2014, for a total of 59 quarters,

we found that the parameters of a sizable fraction of banks lie in the dynamical core region of the parameter space and that the large banks' leverage tends to be more chaotic than the one of small ones. The latter finding was corroborated also by using a non-parametric approach.

We believe that the proposed methodologies may offer revealing perspectives for future works. For instance, it would be interesting to extend the employed mathematical techniques to study a model in which more than one asset and one bank are present in the system.

11 Acknowledgements

This research was supported by the research project 'Dynamics and Information Research Institute - Quantum Information, Quantum Technologies' within the agreement between UniCredit Bank and Scuola Normale Superiore. F.L. and S.M. acknowledge partial support by the European Program scheme 'INFRAIA-01-2018-2019: Research and Innovation action', grant agreement #871042 'So-BigData++: European Integrated Infrastructure for Social Mining and Big Data Analytics'. S.V. is grateful to the Centro di Ricerca Matematica Ennio de Giorgi, Scuola Normale Superiore, Laboratoire International Associé LIA LYSM, the INdAM (Italy) and the UMI-CNRS 3483, Laboratoire Fibonacci (Pisa), where this work has been initiated and completed under a CNRS delegation, for the support. S.V. thanks C. Gonzalez-Tokman for useful discussion about Section 6.3.

A The Chaos Decision Tree Algorithm

The Chaos Decision Tree Algorithm [57] is a non-parametric chaos-detection tool which has been developed with the goal of being especially robust to measurement noise. It provides an automated processing pipeline which has been showed to be able to detect the presence (or absence) of chaos in noisy recordings, even for difficult edge cases. We use it in our work to identify periodic/chaotic time series without any reference to our model. It is meant to provide an independent check on the existence of chaotic behaviour in leverage time series and to support the evidence that it may depend on the bank's size.

The algorithm classifies a time-series as either stochastic or periodic, or chaotic. We now briefly explain how the algorithm works. The first step is to test if data are stochastic. This is done via surrogate-based approach by comparing the permutation entropy of the original time-series to the permutation entropy of random surrogates of that time-series by using a combination of Amplitude Adjusted Fourier Transform surrogates and Cyclic Phase Permutation surrogates. If the permutation entropy of the original time-series falls within either surrogate distribution, the time-series is classified as stochastic. If the permutation entropy falls outside the surrogate distribution, then the algorithm proceeds to de-noise the inputted signal by using the Schreiber's noise-reduction

algorithm [55]. Notice that the calculation of the permutation entropy relies on two parameters: the permutation order and the time-lag. The time-lag has been set to 1 as suggested in [57]. The choice of the order of the permutation is made in order to maximize the detection of chaotic series in our model.

To test the CDTA algorithm on our model, we first consider the deterministic map and generate 100 chaotic and 100 periodic time-series of length 59 from the dynamical core. We then apply CDTA to these series for different values of the permutation order ($\in \{3, \dots, 8\}$). While the periodicity accuracy is maximized for a value equal to 8 (92% of the periodic series are correctly detected as such and the remaining 8% are labeled chaotic), the chaos detection accuracy is maximized for a choice of the permutation order equal to 5 (65% of the series are correctly detected as chaotic and the remaining periodic). Because of the purpose of this paper, we fix the permutation order to 5, but we have checked that the conclusions of our data analysis (in particular Table 4) would have been the same with a different choice.

At this point, the algorithm checks for signal oversampling and, if the data are over-sampled, the algorithm iteratively down-samples the data until they are no longer over-sampled. Finally, CDTA performs the 0-1 chaos test [34] on the input data. Ref. [57] points out that the 0-1 chaos test has been modified from the original one to be less sensitive to noise. Then, it suppresses the correlations arising from quasi-periodicity, and normalizes the standard deviation of the test signal. The value for the parameter that suppresses signal correlations is chosen based on ROC analyses. The modified 0-1 test provides a single statistic, K , which approaches 1 for chaotic systems and approaches 0 for periodic systems. The algorithm sets up a cutoff for K based on the length of the time-series. If K is greater than the cutoff, the data are classified as chaotic, and if they are smaller than or equal to the cutoff, they are classified as periodic.

A.1 Simulations

In this section we present some numerical investigations showing how CDTA performs when simulating (noisy) time-series from the map described in Section 3.4. Specifically, we run the following two numerical experiments:

- (i) First, we simulate time-series from the dynamical core area (i.e. time-series for which the pairs (ϕ^*, ω) satisfy condition (C3): $T(\Delta) < c < \Delta < 1$). More precisely, we simulate 500 samples of different length and level of noise, which is captured by the variable n .
- (ii) Second, we simulate time-series from outside the dynamical core area (the map T thus satisfies (C1) or (C2)). The remaining simulation setting coincides with that in (i).

The procedures explained in (i)–(ii) are also repeated when T is replaced by its k -th iterate T^k , $k = 2, 3$; see discussion in Section 8. Table 4 collects the results. We observe that when both n and the time series length are large, CDTA classifies almost all the time series in the dynamical core as chaotic,

Iterate	Series length	n	Dynamical core			Not dynamical core		
			S (%)	P (%)	C (%)	S (%)	P (%)	C (%)
1	59	5	33.5	5.14	61.4	57.4	4.81	37.7
		20	29.3	4.28	66.5	69.9	3.28	26.8
		100	24.3	6.99	69.6	88.1	2.94	8.97
	295	5	2.2	1.7	96.1	22.5	6.24	71.2
		20	0.1	1.9	98	43.8	10.4	45.8
		100	0	2.3	97.7	73.8	8.35	17.9
	590	5	0	0.7	99.3	13.1	6.08	80.9
		20	0	0.4	99.6	33.6	8.5	57.9
		100	0	0.4	99.6	66.4	8.04	25.6
	1180	5	0	0.1	99.9	10.9	3.44	85.6
		20	0	0	100	27.7	5.57	66.8
		100	0	0	100	60.2	5.29	34.5
2	59	5	75.7	2.17	22.2	83.8	1.33	14.9
		20	80.1	1.65	18.2	92.8	0.26	6.91
		100	86.6	1.43	11.9	96.6	0.56	2.81
	295	5	39.4	0	60.6	40.5	3.26	56.2
		20	38.6	0.6	60.8	70	3.7	26.3
		100	21	1.2	77.8	83.9	2.96	13.1
	590	5	27.6	0	72.4	25.6	3.23	71.2
		20	10.6	0	89.4	52.3	4.24	43.4
		100	4.8	0.6	94.6	74.7	2.88	22.4
	1180	5	11	0	89	13.7	2.22	84.1
		20	0.2	0	99.8	39.4	2.82	57.7
		100	0.2	0	99.8	64.1	2.24	33.7
3	59	5	85.3	0.47	14.2	83.9	1.33	14.9
		20	84.5	1.17	14.3	92.8	0.26	6.91
		100	89.5	1.43	8.79	96.6	0.56	2.81
	295	5	36	0	64	40.5	3.26	56.2
		20	32.6	0.4	67	70	3.7	26.3
		100	23	1.6	75.4	83.9	2.96	13.1
	590	5	20.6	0	79.4	25.6	3.23	71.2
		20	9.6	0	90.4	52.3	4.24	43.4
		100	9.4	0.8	89.8	74.7	2.88	22.4
	1180	5	6	0	94	13.7	2.22	84.1
		20	2	0	98	39.4	2.82	57.7
		100	2.8	0.8	96.4	64.1	2.24	33.7

Table 4: Percentage of time-series detected by the Chaos Decision Tree Algorithm as stochastic (S), periodic (P) and chaotic (C) in the dynamical core and its complement as a function of the time-series length and n for different iterates of the map.

while those outside it are never classified as such. This is quite independent on k . By decreasing either n or the time series length, the classification is less precise and this effect is stronger for larger values of k . In the regime of length comparable with our empirical data ($N = 59$), roughly a third (for $k = 1$) or up to 85% (for $k = 3$) of the time series in the dynamical core are classified as stochastic, showing the limits of the CDTA when the time series are short and/or the noise is large.

References

- [1] Viral V. Acharya and Stephen G. Ryan. “Banks’ Financial Reporting and Financial System Stability”. In: *Journal of Accounting Research* 54.2 (2016), pp. 277–340.
- [2] Tobias Adrian and Hyun Song Shin. “Liquidity and leverage”. In: *Journal of Financial Intermediation* 19.3 (2010), pp. 418–437.
- [3] Tobias Adrian and Hyun Song Shin. “Procyclical Leverage and Value-at-Risk”. In: *The Review of Financial Studies* 27.2 (2013), pp. 373–403.
- [4] Romain Aimino, Matthew Nicol, and Sandro Vaienti. “Annealed and quenched limit theorems for random expanding dynamical systems”. In: *Probability Theory and Related Fields* 162.1-2 (2015), pp. 233–274.
- [5] Jose F. Alves and Vitor Araújo. “Random perturbations of nonuniformly expanding maps”. In: *Astérisque* 286 (2003), pp. 25–62.
- [6] Vitor Araújo. “Attractors and time averages for random maps”. In: *Annales de l’Institut Henri Poincaré (C) Non Linear Analysis* 17.3 (2000), pp. 307–369.
- [7] Vitor Araújo and Ali Tahzibi. “Stochastic stability at the boundary of expanding maps”. In: *Nonlinearity* 18.3 (2005), p. 939.
- [8] Christoph Aymanns and J. Doyne Farmer. “The dynamics of the leverage cycle”. In: *Journal of Economic Dynamics and Control* 50 (2015), pp. 155–179.
- [9] Christoph Aymanns et al. “Taming the Basel leverage cycle”. In: *Journal of Financial Stability* 27 (2016), pp. 263–277.
- [10] Wael Bahsoun, Huyi Hu, and Sandro Vaienti. “Pseudo-Orbits, Stationary Measures and Metastability”. In: *Dynamical Systems* 29.3 (2014), pp. 322–336.
- [11] Viviane Baladi. *Positive Transfer Operators and Decay of Correlations*. Vol. 14. World Scientific, 2000.

- [12] Viviane Baladi, Michael Benedicks, and Véronique Maume-Deschamps. “Almost sure rates of mixing for iid unimodal maps”. In: *Annales Scientifiques de l’Ecole Normale Supérieure* 35.1 (2002), pp. 77–126.
- [13] Viviane Baladi and Marcelo Viana. “Strong stochastic stability and rate of mixing for unimodal maps”. In: *Annales Scientifiques de l’Ecole Normale Supérieure* 29.4. (1996), pp. 483–517.
- [14] Nils Berglund and Barbara Gentz. *Noise-induced phenomena in slow-fast dynamical systems: a sample-paths approach*. Springer Science & Business Media, 2006.
- [15] Rabindra N. Bhattacharya and Mukul Majumdar. *Random Dynamical Systems: Theory and applications*. Cambridge, 2007.
- [16] Alexander Blokh and Mikhail Lyubich. “Measurable dynamics of S-unimodal maps of the interval”. In: *Annales scientifiques de l’Ecole normale supérieure* 24.5 (1991), pp. 545–573.
- [17] Aleksandr A. Borovkov. *Ergodicity and Stability of Stochastic Processes*. J. Wiley, 1998.
- [18] Abraham Boyarsky and Pawel Gora. *Laws of Chaos: Invariant Measures and Dynamical Systems in One Dimension*. Birkhäuser, 1997.
- [19] Anne Broise. “Transformations dilatantes de l’intervalle et théorèmes limites”. In: *Asterisque-societe mathematique de France* 238 (1996), pp. 1–109.
- [20] Giuseppe Castellacci and Youngna Choi. “Modeling contagion in the Eurozone crisis via dynamical systems”. In: *Journal of Banking & Finance* 50 (2015), pp. 400–410.
- [21] Sheng Chen and Stephen A. Billings. “Neural networks for nonlinear dynamic system modelling and identification”. In: *International Journal of Control* 56.2 (1992), pp. 319–346.
- [22] Sheng Chen, Stephen A. Billings, and Peter Grant. “Non-linear system identification using neural networks”. In: *International Journal of Control* 51.6 (1990), pp. 1191–1214.
- [23] Youngna Choi and Raphael Douady. “Financial crisis dynamics: attempt to define a market instability indicator”. In: *Quantitative Finance* 12.9 (2012), pp. 1351–1365.
- [24] Youngna Choi, Raphael Douady, et al. “Financial crisis and contagion: A dynamical systems approach”. In: *Handbook on systemic risk* (2013), pp. 453–479.

- [25] Fulvio Corsi, Stefano Marmi, and Fabrizio Lillo. “When micro prudence increases macro risk: The destabilizing effects of financial innovation, leverage, and diversification”. In: *Operations Research* 64.5 (2016), pp. 1073–1088.
- [26] Jón Daniélsson, Hyun Song Shin, and Jean-Pierre Zigrand. “Procyclical Leverage and Endogenous Risk”. In: *Available at SSRN, abstract=1360866* (2012).
- [27] Jón Daniélsson, Hyun Shin, and Jean-Pierre Zigrand. “The impact of risk regulation on price dynamics”. In: *Journal of Banking & Finance* 28.5 (2004), pp. 1069–1087.
- [28] Domenico Di Gangi, Fabrizio Lillo, and Davide Pirino. “Assessing systemic risk due to fire sales spillover through maximum entropy network reconstruction”. In: *Journal of Economic Dynamics and Control* 94 (2018), pp. 117–141.
- [29] Dmitrii I. Dolgopyat. “Averaging and invariant measures”. In: *Moscow Mathematical Journal* 5.3 (2005), pp. 537–576.
- [30] Ana Fostel and John Geanakoplos. “Leverage cycles and the anxious economy”. In: *American Economic Review* 98.4 (2008).
- [31] Stefano Galatolo, Maurizio Monge, and Isaia Nisoli. “Existence of Noise Induced Order, a Computer Aided Proof”. In: *Nonlinearity* 33.9 (2020), p. 4237.
- [32] Quentin Gai, Gianetto, Jean-Marc Le Caillec, and Erwan Marrec. “Estimating the predictability of economic and financial time series”. In: *arXiv:1212.2758v1* (2012).
- [33] Ian Goodfellow, Yoshua Bengio, and Aaron Courville. *Deep Learning*. MIT Press, 2016.
- [34] Georg A. Gottwald and Ian Melbourne. “On the implementation of the 0–1 test for chaos”. In: *SIAM Journal on Applied Dynamical Systems* 8.1 (2009), pp. 129–145.
- [35] Harry Huizinga and Luc Laeven. “Bank valuation and accounting discretion during a financial crisis”. In: *Journal of Financial Economics* 106.3 (2012), pp. 614–634.
- [36] Gerhard Keller. “Exponents, attractors and Hopf decompositions for interval maps”. In: *Ergodic Theory and Dynamical Systems* 10.4 (1990), pp. 717–744.
- [37] Yuri Kifer. *Ergodic Theory of Random Transformations*. Springer, 1986.
- [38] Diederik P. Kingma and Jimmy Ba. “Adam: A Method for Stochastic Optimization”. In: *arXiv:1412.6980* (2014).

- [39] Leonid Korolov and Yakov Sinai. *Theory of Probability and Random Processes*. Springer, 2012.
- [40] Yann LeCun et al. “Object Recognition with Gradient-Based Learning”. In: *Shape, Contour and Grouping in Computer Vision* (1999).
- [41] Bárbara Llacay and Gilbert Peffer. “Impact of value-at-risk models on market stability”. In: *Journal of Economic Dynamics and Control* 82 (2017), pp. 223–256.
- [42] Andrzej Materka. “Application of artificial neural networks to parameter estimation of dynamical systems”. In: *Conference Proceedings. 10th Anniversary. IMTC/94. Advanced Technologies in I & M. 1994 IEEE Instrumentation and Measurement Technology Conference (Cat. No. 94CH3424-9)* (1994), pp. 123–126.
- [43] Kenji Matsumoto and Ichiro Tsuda. “Noise-induced Order”. In: *Journal of Statistical Physics* 31.1 (1983), pp. 87–106.
- [44] Piero Mazzarisi, Fabrizio Lillo, and Stefano Marmi. “When panic makes you blind: A chaotic route to systemic risk”. In: *Journal of Economic Dynamics and Control* 100 (2019), pp. 176–199.
- [45] Wellington de Melo and Sebastian van Strien. *One-Dimensional Dynamics*. Vol. 25. Springer Science & Business Media, 2012.
- [46] Sean P. Meyn and Richard L. Tweedie. *Markov Chains and Stochastic Stability*. Springer-Verlag, 1993.
- [47] Kumpati S. Narendra and Kannan Parthasarathy. “Identification and control of dynamical systems using neural networks”. In: *IEEE Transactions on Neural Networks* 1.1 (1990), pp. 4–27.
- [48] Isaia Nisoli. “Sufficient conditions for Noise Induced Order in 1-dimensional systems”. In: *arXiv:2003.08422* (2020).
- [49] Tomasz Nowicki and Sebastian van Strien. “Invariant measures exist under a summability condition for unimodal maps”. In: *Inventiones Mathematicae* 105.1 (1991), pp. 123–136.
- [50] Galo Nuño and Carlos Thomas. “Bank Leverage Cycles”. In: *American Economic Journal: Macroeconomics* 9.2 (2016), pp. 37–72.
- [51] Avinash Persaud. “Sending the herd off the cliff edge: the disturbing interaction between herding and market-sensitive risk management practices”. In: *Journal of Risk Finance* 2.1 (2000), pp. 59–65.
- [52] Sebastian Poledna et al. “Leverage-induced systemic risk under Basel II and other credit risk policies”. In: *Journal of Banking & Finance* 42 (2014), pp. 199–212.

- [53] Jitendra R. Raol and Himesh Madhuranath. “Neural network architectures for parameter estimation of dynamical systems”. In: *IEE Proceedings: Control Theory and Applications* 143.4 (1996), pp. 387–394.
- [54] David Ruelle. “An inequality for the entropy of differentiable maps”. In: *Bol. Soc. Bras. Mat.* 9 (1978), pp. 83–87.
- [55] Thomas Schreiber. “Extremely simple nonlinear noise-reduction method”. In: *Physical Review E* 47.4 (1993), p. 2401.
- [56] Hans Thunberg. “Periodicity versus Chaos in One-Dimensional Dynamics”. In: *SIAM Review* 43.1 (2001), pp. 3–30.
- [57] Daniel Toker, Friedrich T. Sommer, and Mark D’Esposito. “A simple method for detecting chaos in nature”. In: *Communications Biology* 3.1 (2020), pp. 1–13.
- [58] Marcelo Viana. *Stochastic Dynamics of Deterministic Systems*. Brazillian Math. Colloquium, IMPA, 1997.
- [59] Xubin Zeng, Roger A. Pielke, and Richard Eykholt. “Extracting Lyapunov exponents from short time series of low precision”. In: *Modern Physics Letters B* 6.02 (1992), pp. 55–75.